UNIVERSITY OF OKLAHOMA

GRADUATE COLLEGE

# EXPERIMENTAL INVESTIGATION OF SYNTHETIC AND MICROBIAL SURFACTANTS FOR ENHANCED OIL RECOVERY IN BONE SPRING SANDSTONES

A THESIS

SUBMITTED TO THE GRADUATE FACULTY

in partial fulfillment of the requirements for the

Degree of

MASTER OF SCIENCE

By

RISHABH PANDEY
Norman, Oklahoma
2022

Downloaded from SHAREOK. Persistent Handle URL: https://hdl.handle.net/11244/336904

EXPERIMENTAL INVESTIGATION OF SYNTHETIC AND MICROBIAL SURFACTANTS FOR ENHANCED OIL RECOVERY IN BONE SPRING SANDSTONES

A THESIS APPROVED FOR THE

MEWBOURNE SCHOOL OF PETROLEUM AND GEOLOGICAL ENGINEERING

BY THE COMMITTEE CONSISTING OF

Dr. Chandra S. Rai, Chair

Dr. Deepak Devegowda

Dr. Benjamin Shiau

© Copyright by RISHABH PANDEY 2022
All Rights Reserved.

**Acknowledgments**

I would like to thank my advisor, Dr. Chandra Rai, for giving me this opportunity to pursue research under his guidance. His support and guidance have helped me grow professionally and personally. I am highly thankful to Dr. Ali Tinni, Dr. Carl Sondergeld, Dr. Deepak Devegowda, and Dr. Benjamin Shiau for their valuable inputs towards my research and academics.

I would like to thank Dr. Mark Curtis for his mentorship and helping me become a better researcher. I would also like to thank fellow $IC^3$ colleagues, especially Gary, for all his help. I would also like to thank Kachi and Dr. Mandeep Kaur from Applied Surfactant Laboratory for taking the time to train me on equipment in their lab.

Finally, I would like to thank my parents and family for their unconditional support and love. Special shoutout to my friends Akshay and Laura, whom I met here at OU, for making this journey fun.

## Table of Contents

Acknowledgments ..... iv
Table of Contents ..... v
List of Figures ..... vii
List of Tables ..... xi
Abstract ..... xii
Chapter 1 : Introduction ..... 1
1.1 Organization of the Thesis ..... 2
Chapter 2 : Literature Review ..... 4
2.1 Oil Recovery ..... 4
2.2 Enhanced Oil Recovery ..... 4
2.3 Wettability ..... 5
2.4 Surfactant Flooding ..... 6
2.5 Types of Surfactants ..... 6
2.5 Wettability Alteration Mechanisms ..... 7
2.5.1 Ion Pair Formation Mechanism ..... 8
2.5.2 Surfactant Adsorption Mechanism ..... 8
2.6 Critical Micelle Concentration ..... 9
2.7 Surfactant Adsorption and Imbibition Studies using Synthetic Surfactants ..... 10
2.8 Surfactant Adsorption, Wettability Alteration, and Imbibition Studies using Biosurfactants ..... 12
Chapter 3 : Measurement Procedures ..... 14
3.1 Petrophysical Analysis ..... 14
3.1.1 Mineralogy Measurements ..... 14
3.1.2 Porosity Measurements ..... 15
3.1.3 Total Organic Content Measurements ..... 15
3.2 Fluid Characterization ..... 15
3.2.1 Density Measurements ..... 16
3.2.2 Surfactant Stability Tests ..... 16
3.2.3 Critical Micelle Concentration Measurements ..... 16
3.2.4 Interfacial Tension Measurements ..... 18
3.3 Contact Angle Measurements ..... 19

3.4 Surfactant Adsorption Measurements ..... 20
3.5 Imbibition Experiments using Produced Brine and Surfactants ..... 23
3.6 Determination of Water and Oil Region in NMR T1-T2 Maps ..... 29
Chapter 4 : Results and Discussion ..... 31
4.1 Petrophysical Analysis ..... 31
4.2 Fluid Characterization ..... 32
4.2.1 Density Measurements ..... 32
4.2.2 Surfactant Stability Tests ..... 33
4.2.3 pH Measurements ..... 34
4.2.4 ICP Analysis: Before Imbibition Experiments ..... 34
4.2.3 Critical Micelle Concentration Measurements ..... 36
4.2.4 Interfacial Tension Measurements ..... 37
4.3 Contact Angle Measurements ..... 37
4.4 Surfactant Adsorption Measurements ..... 40
4.5 Relationship between Surfactant Adsorption and Mineralogy ..... 46
4.5.1 Surfactant Adsorption Relationship with Quartz plus Feldspars ..... 46
4.5.2 Surfactant Adsorption Relationship with Clays ..... 47
4.5.3 Surfactant Adsorption Relationship with Carbonates ..... 48
4.6 Imbibition Experiments using Produced Brine and Surfactants ..... 49
Chapter 5 : Conclusions, Surfactant Selection Strategy and Future Work Recommendations ..... 53
5.1 Conclusions ..... 53
5.2 Surfactant Selection Strategy for Sandstones ..... 54
5.3 Future Work Recommendations ..... 55
References ..... 57

## List of Figures

Figure 1 - Force balance on water-oil-rock system (Standnes 2001). ..... 5

Figure 2 - General structure of surfactant molecule. ..... 7

Figure 3 - Model showing wettability alteration. (a) ion-pair formation mechanism, and (b) surfactant adsorption mechanism (Standnes & Austad 2000; Bashir et al. 2021). ..... 9

Figure 4 - Surface tension variation with increase in surfactant concertation (Kruss 2022). ..... 10

Figure 5 - Step by step experimental workflow for surfactant adsorption measurements used in this study. ..... 23

Figure 6 - Experimental setup used in this study to imbibe plug samples in produced brine and surfactant solutions. ..... 26

Figure 7 - Step by step experimental workflow for produced brine and surfactant imbibition measurements used in this study. ..... 26

Figure 8 - NMR T1-T2 maps of sandstone samples pre and post-imbibition using produced brine. (a) shows bound fluid inside the sample after cleaning and drying, (b) shows the total volume of total fluid inside the sample (crude oil plus bound fluid) after oil saturation with one signal relaxing elongated over T1/T2 ratio due to presence of hydrocarbons with varying carbon number, and (c) showing two main signals relaxing at different T1/T2 ratios which indicate presence of two different fluids inside the sample. Highlighted region here shows oil present inside the sample post-imbibition. ..... 27

Figure 9 - NMR T2 measurements of three samples saturated with oil before imbibition. T2 spectra here show two peaks, with second peak having higher amplitude showing oil inside the sample. With all the T2 spectra overlapping each other very closely, we can say that the sample reached similar initial oil saturation. ..... 28

Figure 10 - NMR T1-T2 map showing two signals relaxing at different T1/T2 ratios after imbibition with produced brine, pre-surfactant 1. ..... 29
Figure 11 - NMR T1-T2 maps of sandstone sample after imbibition with NMR doping agent. Post imbibition with brine, sample shows two signals relaxing at different T1/T2 ratios. To distinguish water and oil signal and to quantify oil recovery, sample was imbibed in $D_2O$ for 8 days. With time we see a decrease in amplitude of signal having faster relaxation, which shows it is water, while the signal having slower relaxation remains the same, which shows it is oil. ..... 30
Figure 12 - Surfactant stability tests shows surfactants are stable at 2 gpt concentration as the solutions remained transparent after 3 days at 70$^o$F and 145$^o$F. ..... 33
Figure 13 - IFT measurement of produced brine and three surfactants at 2 gpt concentration. ... 34
Figure 14 - ICP analysis of produced brine and surfactant solution at 2 gpt concentration showing major ion constituents. ..... 35
Figure 15 - Surface tension at variable surfactant concentration for CMC measurement. ..... 36
Figure 16 - IFT measurement of produced brine and surfactants at 2 gpt concentration. ..... 37
Figure 17 - Contact angle measurements between sandstone samples and surfactants at 2 gpt concentration along with produced brine used in this study. Measurements post oil saturation shows all the samples are oil-and-intermediate wet. After imbibition with brine, the sample remains intermediate wet. With surfactants, the samples become water wet. ..... 39
Figure 18 - Model showing ion-pair formation using oil-wet sandstone samples. ..... 39
Figure 19 - Schematic illustration of the adsorption mechanism at water-clay interface (Liu et al. 2019). ..... 40
Figure 20 - Light absorption spectrum for surfactant solutions measured at varying concentrations using UV-Vis spectrophotometer. ..... 42

Figure 21 - Calibration curves for surfactants used in this study. Here recorded light absorptions were plotted at peak absorption wavelength of 240 nm at varying surfactant concentrations for three surfactants. ..... 43

Figure 22 - Light absorption spectrum for surfactant solutions post imbibition at 2 gpt concentration using UV-Vis spectrophotometer. ..... 43

Figure 23 - Surfactant adsorption results at 2 gpt concentration using UV-Vis spectrophotometer. ..... 44

Figure 24 - Model showing ion-pair formation between polar head of amphoteric surfactant and sandstone surface. ..... 44

Figure 25 - Adsorption of negative charged polar head of amphoteric surfactant to clay surface with $Ca^{2+}$ as a cationic bridge (Liu et al. 2021). ..... 45

Figure 26 - Excess $Ca^{2+}$ ions in surfactant solution creates multilayer of adsorped amphoteric surfactant (Liu et al. 2021). ..... 45

Figure 27 - Model showing reduction in electrostatic repulsion between same charge on polar head of surfactants due to presence of divalent cations. ..... 45

Figure 28 - Surfactant adsorption results for five samples at 2 gpt concentration using UV-Vis spectrophotometer. ..... 46

Figure 29 - Relationship between amphoteric and biosurfactant adsorption with quartz plus feldspars in Bone Spring Sandstones. ..... 47

Figure 30 - Relationship between amphoteric and biosurfactant adsorption with total clays (illite plus mixed clays) in Bone Spring sandstones. ..... 48

Figure 31 - Relationship between amphoteric and biosurfactant adsorption with total carbonates (dolomite plus calcite) in Bone Spring sandstones. ..... 49

Figure 32 - Oil recovery measured experimentally using imbibition of produced brine and surfactants at 2 gpt concentration in three Bone Spring sandstone samples at 500 psi and 145ºF. All three samples were exposed to brine and surfactants in a series of tests, as shown in Table 1. 12 MHz NMR was used to quantify the oil recovery by calculating the volume of oil inside the sample before and after imbibition. ..... 51
Figure 33 - Average oil recovery measured experimentally using imbibition of produced brine and surfactants at 2 gpt concentration on three Bone Spring sandstone samples at 500 psi and 145ºF. ..... 51

## List of Tables

Table 1 - Test matrix showing imbibition measurements performed on same three samples in testing order to quantify the oil recovery. ..... 28

Table 2 - Mineralogy, TOC, and porosity of Bone Spring sandstone samples used in this study for imbibition experiments. ..... 31

Table 3 - Mineralogy of Bone Spring sandstone samples used in this study to analyze relationship between surfactant adsorption and mineralogy. ..... 31

Table 4 - Description of different surfactants used in this study. ..... 32

Table 5 - Density of crude oil at 145$^{o}$F along with produced brine, and surfactant solutions at 2 gpt concentration and 70$^{o}$F. ..... 33

Table 6 - Ion analysis of produced brine. ..... 35

Table 7 - CMC measurements of surfactants used in this study. ..... 36

Table 8 - Summary of IFT, contact angle, surfactant adsorption, and oil recovery experiment results using produced brine and surfactants at 2 gpt concentration. ..... 52

## Abstract

Surfactants have been used to increase hydrocarbon recovery to meet the increasing demand for oil and gas. This mechanism of using surfactants reduces the Interfacial Tension (IFT) at the fluid/fluid interface and wettability at the rock/fluid interface to mobilize trapped oil out of the pores. However, there are two main limitations of the surfactant flooding process—first, high reservoir temperature & salinity, and second, adsorption of surfactants on the rock surface. Surfactant adsorption alters wettability of reservoir rock from oil-wet to water-wet. However, excess adsorption may decrease oil recovery, especially in conventional reservoirs with high temperature and Total Dissolved Solids (TDS).

This study tested two synthetic amphoteric surfactants, one nonionic biosurfactant, and a base case with produced brine to understand wettability, IFT, surfactant adsorption, and its effect on oil recovery in Bone Spring sandstone formation. Produced brine has a high TDS of 237,705 ppm, and test conditions were kept at 145$^{o}$F and 500 psi pressure. First, surfactant stability tests and CMC measurements were performed on three surfactants. Then, IFT measurements were performed between crude oil and surfactant solutions along with produced brine. Next, wettability alteration was studied by measuring contact angle on oil saturated rock samples before and after being exposed with surfactants and produced brine. Then, surfactant adsorption experiments were performed using UV-Vis spectrophotometer to calculate the amount of surfactant getting adsorbed on the rock samples. Lastly, surfactants and brine imbibition experiments were performed on plug samples, and oil recovery was quantified using 12MHz Nuclear Magnetic Resonance (NMR) spectrometer. All the recovery experiments were repeated on the same three plug samples with approximately 30 wt.% clay.

This study shows that all three surfactants reduced IFT and altered wettability, but biosurfactant showed low IFT, much lower surfactant adsorption, and made the sample most water wet as compared to amphoteric surfactants. Imbibition experiments showed that biosurfactant have the highest oil recovery, while amphoteric surfactants have oil recovery even lower than produced brine. This study shows that surfactant adsorption affects oil recovery, which leads to loss of surfactants from solution to the rock surface. Measurements also show that the adsorption of amphoteric surfactants increases with increased clay concentration which shows the efficacy of surfactants depends on rock mineral composition.

This study suggests that biosurfactants with glycolipids can be used in shaly sandstones at high TDS and temperature. With oil recovery using biosurfactants being very close to produced brine, it might be more economical to use only produced brine with no surfactants.

## Chapter 1 : Introduction

To meet the ever increasing demand for oil & gas and to keep the hydrocarbon exploration & production business economical, it is essential to improve recovery from depleting oil & gas reservoirs. Primary and secondary recovery methods in conventional reservoirs result in 10 to 35% recovery of the Original Oil in Place (OOIP) (Ali and Stahl, 1970). Tertiary recovery or Enhanced Oil Recovery (EOR) methods are used to increase the recovery to 60% or more of the OOIP.

One of the most extensively used EOR processes to reduce oil saturation is injection of chemicals into the reservoir, known as surfactant flooding. Studies have shown that different types of surfactants, including anionic, cationic, nonionic, and amphoteric, can increase oil recovery (Lake 1989 and Schramm 2000). Besides synthetic surfactants, biosurfactants synthesized from enzymes and microorganisms are also commercially available. Studies have shown that the imbibition of synthetic or biosurfactants in conventional reservoirs alters the wettability of rock to water-wet (Saxena et al. 2017; Kumar and Mandal 2019). These surfactants reduce the Interfacial Tension (IFT) at fluid-fluid interface and mobilize trapped oil out of the pores. This mechanism of using surfactants increases the capillary number by reducing the capillary forces, which depends on IFT and contact angle.

Surfactant flooding process has two main limitations—first, high reservoir temperature & high salinity, and second, excess adsorption of surfactants on the rock surface, which can reduce the recovery of trapped oil from pores inside the rocks. Numerous studies have identified various reasons for surfactant adsorption, which include ion exchange, ion association, hydrophobic bonding, dispersion forces, electrostatic attraction, van der Waals forces, and polarization of $\pi$ electrons (Paria and Khilar 2004; Zhang and Somasundaran 2006; Dang et al. 2011; Kamal et al. 2017).

Considering the increasing interest of exploration and production companies in using surfactant flooding in shaly sandstones having high TDS and temperature, this study aims to use a set of related experiments to determine the role of surfactants in improving oil recovery using surfactant flooding in Bone Spring sandstone. This study will close the existing gaps in the literature by testing two synthetic surfactants (amphoteric) and one biosurfactant (nonionic) using sandstone plug samples, crude oil, and produced brine from the well site. As per our best knowledge, no literature is currently available with thoroughly performed experiments that evaluates the use of surfactants, especially nonionic biosurfactant, to understand wettability, IFT, surfactant adsorption, and its effect on oil recovery in shaly sandstones.

This study uses a set of related experiments to understand the combined effect of IFT and wettability on oil recovery with a focus on surfactant adsorption using samples from Bone Spring sandstone. The specific objectives are described as follows:

a) Investigate the effect of amphoteric and biosurfactants on IFT using produced brine having high TDS.
b) Investigate the effect of amphoteric and biosurfactants on wettability alteration and oil recovery in shaly sandstone at high TDS and temperature
c) Determine surfactant adsorption during imbibition and correlate it with surfactant type, rock mineralogy, and oil recovery.

### 1.1 Organization of the Thesis

The rest of thesis is divided into four additional chapters and is organized as follows:

Chapter 2 introduces a literature review on the fundamentals of oil recovery, wettability, surfactant flooding, and wettability alteration mechanisms. This section also describes the state-of-art on

surfactant adsorption, wettability alteration, and imbibition using synthetic and microbial surfactants in sandstones.

Chapter 3 describes the experimental methodologies used for petrophysical analysis, fluid characterization, wettability alteration, surfactant adsorption, and imbibition on Bone Spring sandstones using produced brine and surfactants.

Chapter 4 describes the findings of this study with a focus on understanding the low oil recovery of amphoteric surfactants as compared to produced brine using surfactant adsorption measurements.

Chapter 5 presents the conclusions, surfactant selection strategy for sandstones, and future work recommendations.

# Chapter 2 : Literature Review

## 2.1 Oil Recovery

The process of increasing recovery is divided into three major phases: primary, secondary, and tertiary (Green and Willhite 1998). Primary recovery, which depends on natural energy of the reservoir, produces less than 30% of the Original Oil in Place (OOIP). As the pressure gradient in the reservoir falls, production also decreases. Then secondary recovery methods are deployed in which water and gas are injected into the reservoir to increase the natural energy. Water flooding is the most common secondary recovery method in which water is injected into the reservoir using several injection wells, and oil is produced using producer wells. This method also doesn't recover all the oil as water cannot reach everywhere due to reservoir heterogeneity and has low displacement sweep efficiency. Then tertiary recovery or Enhanced Oil Recovery (EOR) methods are used. These methods increase the recovery to 60% or more of the OOIP.

## 2.2 Enhanced Oil Recovery

In conventional reservoirs, EOR methods reduce remaining oil saturation after primary and secondary recovery phases. This reduction in saturation depends on displacement efficiency (Eq.1)

$$E = E_D * E_V \tag{1}$$

where $E$ = displacement efficiency; $E_D$ = microscopic displacement efficiency; and $E_V$ = macroscopic displacement efficiency.

Capillary forces affect microscopic displacement efficiency. These forces depend on fluid-fluid interactions, such as interfacial tension, and rock-fluid interaction, such as wettability, ion exchange, and surfactant adsorption (Shah and Schechter 1977).

## 2.3 Wettability

Wettability is defined as the affinity of a fluid to spread on a rock surface in presence of second fluid in the system (Anderson 1986). In a water-wet rock, water is the wetting phase and has a higher affinity towards the rock, while oil is the non-wetting phase and is present in center of the pore. Wetting phase fluid occupies small pores, while non-wetting phase fluid occupies larger pores in a water-oil-rock system (Basu & Sharma 1997; Abdullah et al. 2007).

Conventional rocks like sandstone show homogenous wettability as they have uniform mineralogy and significantly less organic content than shales (Wang et al. 2011). Wettability of conventional rocks can be determined by measuring contact angle. These measurements are based on balancing interfacial tension on the surface of water-oil-rock system using Young's equation (Eq. 2), as shown in Figure 1. Rock surface wettability is categorized from 0° to 75° as water-wet, 75° to 105° as intermediate-wet, and 105° to 180° as oil-wet (Anderson 1986).

$$\sigma_{OS} = \sigma_{WS} + \sigma_{OW} * cos\theta \tag{2}$$

where $\sigma_{OS}$ = oil-rock IFT (N/m); $\sigma_{WS}$ = water-rock IFT (N/m); $\sigma_{OW}$ = oil-water IFT (N/m); and $\theta$ = contact angle (degree).

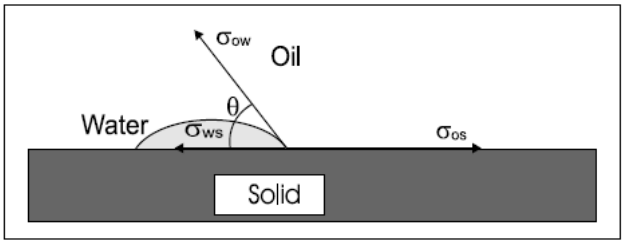



**Figure 1 - Force balance on water-oil-rock system (Standnes 2001).**

## 2.4 Surfactant Flooding

Surfactant flooding is one of the most extensively used chemical EOR process to increase oil recovery. Surfactants reduce interfacial tension and alter wettability to mobilize trapped oil out of the pores. This mechanism of using surfactants increases the capillary number (Eq. 3) by reducing the capillary forces. Reduction in these forces increases the microscopic displacement, thus increasing net oil recovery from the reservoir.

$$N_c = \frac{v * \mu}{\sigma * cos\theta} \tag{3}$$

where $N_c$= capillary number (dimensionless); $v$ = Darcy velocity of the displacing phase (m/s); $\mu$ = pore scale viscosity of the displacing fluid (cP); $\sigma$ = interfacial tension between wetting and non-wetting phase (mN/m); and $\theta$ = contact angle (degree).

## 2.5 Types of Surfactants

For this study, we have classified surfactants based on their origin and composition into two categories: synthetic and microbial/biosurfactants. Surfactants that have been synthesized using chemicals are called synthetic surfactants, while surfactants that have been synthesized from enzymes and microorganisms are called biosurfactants. Structure of these surfactant molecules contains a hydrophilic head group (water-soluble) and a hydrophobic tail (water-insoluble), as shown in Figure 2.

Both of these surfactants can be further classified into four different types depending on the charge in their hydrophilic head as anionic (negative charge), cationic (positive charge), nonionic (no charge), and amphoteric/zwitterionic surfactants (positive and negative charge). Charge on the hydrophilic head of amphoteric surfactants depends on pH of the solution. They

exhibit cationic behavior at acidic pH, anionic behavior at alkaline pH, and nonionic behavior at neutral pH (Schramm 2000; Lake 1989; Honciuc 2021).

Biosurfactants are further classified based on their size as low molecular weight and high molecular weight. Low molecular weight biosurfactants, especially glycolipids, are the interest of our study for EOR as they reduce interfacial tension. High molecular weight biosurfactants stabilize the oil in water emulsions (Paulino et al. 2016). Glycolipids are synthesized from various sources such as microorganisms, hydrocarbons, industrial waste, and oil waste. (Ines and Dhouba, 2015). Components of the cell membrane and certain bacteria are also used to synthesize glycolipids from microorganisms (Velioglu & Urek 2015 and Gunther et al. 2017).

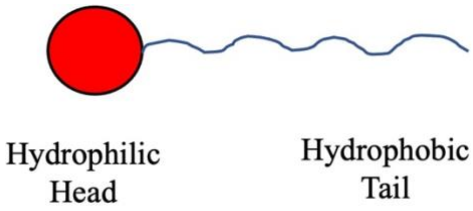



**Figure 2 - General structure of surfactant molecule.**

### 2.5 Wettability Alteration Mechanisms

Various studies have shown that the alteration of reservoir wettability from oil-wet to water-wet depends on three mechanisms:

a) Ion Pair Formation Mechanism

b) Surfactant Adsorption Mechanism

c) Micellar Solubilization Mechanism

In this study, we have focused on ion pair formation and surfactant adsorption to understand the wettability alteration mechanisms for synthetic and biosurfactants in sandstones at high TDS and temperature.

### 2.5.1 Ion Pair Formation Mechanism

The effect of ion pair formation was first explained by Standnes and Austad 2000 using oil-wet outcrop chalk samples and cationic & anionic surfactants. Their experimental results showed that cationic surfactants have higher oil recovery than anionic surfactants in chalk samples. This was explained using a model shown in Figure 3a, which suggests that an ion pair formation occurred between the positively charged head of cationic surfactant and negative charged adsorbed oil molecules. Once the oil from surface was desorbed, chalk became water wet, and imbibition of water gave higher oil recovery.

### 2.5.2 Surfactant Adsorption Mechanism

Standnes and Austad 2000 also explained surfactant adsorption mechanism using oil-wet outcrop chalk samples and cationic & anionic surfactants. Their experimental results showed that anionic surfactants have lower recovery than cationic surfactants. This was explained using a model shown in Figure 3b, which suggests that anionic surfactants created a double layer due to hydrophobic interaction between the negative charged head of the anionic surfactant and negative charged adsorbed oil molecules.

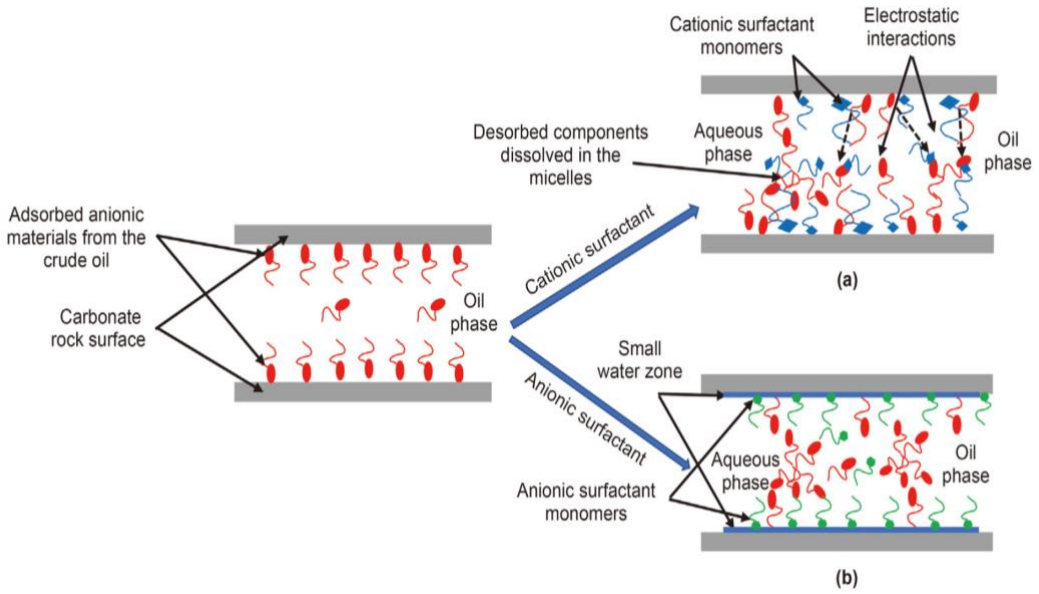



**Figure 3 - Model showing wettability alteration. (a) ion-pair formation mechanism, and (b) surfactant adsorption mechanism (Standnes & Austad 2000; Bashir et al. 2021).**

### 2.6 Critical Micelle Concentration

Surfactants reduce surface tension by getting adsorbed onto the solid surface. Since these surfaces have limited area, these surfactants can only get adsorbed up to a limit. After the limit is reached, excess surfactants start forming micelles and do not reduce surface tension. The concentration of surfactants at which surfactants start forming micelles is called Critical Micelle Concentration (CMC). Below the CMC, surface tension reduces with an increase in surfactant concentration as more and more surfactant gets adsorbed at the surface. Above the CMC, surface tension remains constant with an increase in surfactant concentration, as shown in Figure 4. Measuring CMC for any surfactant solution becomes critical in selecting the right concentration. Any concentration below CMC will not give an effective reduction in IFT and will reduce its efficacy.

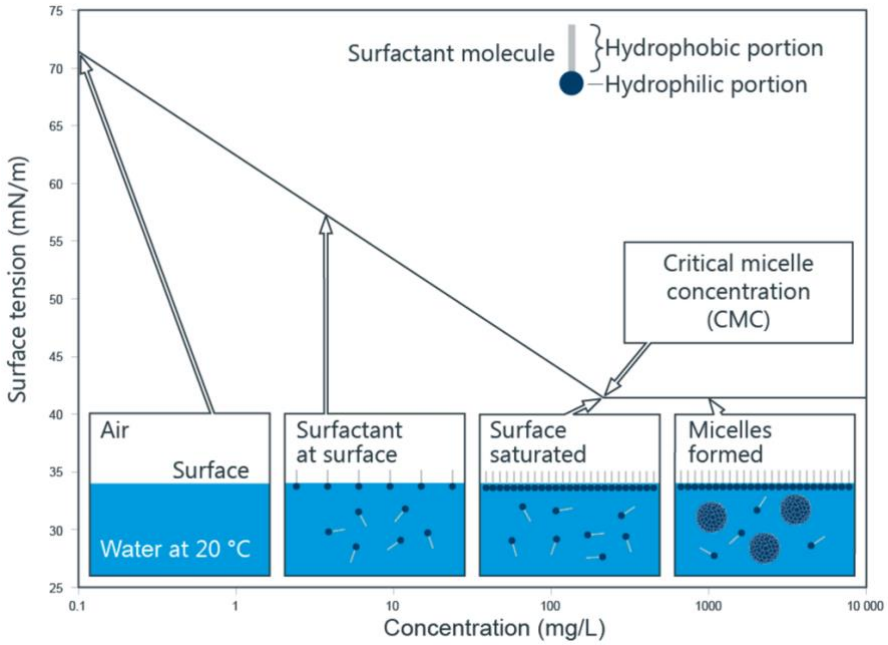



**Figure 4 - Surface tension variation with increase in surfactant concertation (Kruss 2022).**

### 2.7 Surfactant Adsorption and Imbibition Studies using Synthetic Surfactants

Surfactant adsorption decreases surface tension and increases oil recovery, but excess adsorption decreases the effect of surfactant solution as it moves inside the reservoir. This is why it becomes crucial to study surfactant adsorption for every surfactant before doing any field test.

Surfactant adsorption depends on the reactivity between the charge of the surfactant solution and charges on the rock surface, which depends on various factors such as surfactant type, rock mineralogy, surfactant concentration, reservoir temperature, salinity, pressure, and pH (Azam et al. 2014; Baviere et al. 1988; Paria and Khilar 2004; Siracusa and Somasundaran 1987). Numerous studies have identified various reasons for surfactant adsorption between surfactants and rock surface, which include ion exchange, ion association, hydrophobic bonding, dispersion forces, electrostatic attraction, van der Waals forces, and polarization of $\pi$ electrons (Paria and Khilar 2004; Zhang and Somasundaran 2006; Dang et al. 2011; Kamal et al. 2017). For nonionic

surfactants, Nowrouzi et al. 2021 and Paternina et al. 2020 identified hydrogen bonding between the surfactant and hydroxyl group on the rock surface as the main reason for surfactant adsorption.

Anionic surfactants are preferred in sandstone reservoirs as they have least surfactant adsorption due to electrostatic repulsion between the negative charged rock surface and surfactant with negative charged head. Excess adsorption can still occur in sandstones with high illite or kaolinite content, especially in reservoirs with high TDS and temperature. Study on Berea sandstones showed adsorption of 5 mg/gm-rock under high saline environment with TDS greater than 300,000 ppm. The main reason for this adsorption was the presence of high number of cations in brine which gets adsorbed on the rock surface (Budhathoki et al. 2016). Another study on quartz-rich sandstones using anionic surfactant showed that adsorption increases with increase in salinity (Saxena et al. 2019). Study on illite-rich clay samples using anionic surfactants, showed lower adsorption in low and medium-salinity brine (Ingrid 2014).

Along with anionic surfactants, amphoteric surfactants have also been tested in sandstone reservoirs. Adsorption study using two amphoteric surfactants at 95$^{o}$C and 170,000 TDS showed lower IFT and higher oil recovery than brine flooding (Bataweel and Nasr-El-Din, 2012). Study on sandstones (89% quartz and 10% kaolinite) using amphoteric surfactants showed 18.95% higher oil recovery than brine flooding (Kumar and Mandal 2019). Studies have also shown that amphoteric surfactants, as compared to anionic surfactants, have higher stability and solubility at high temperature, high salinity, and wide range of pH conditions (Cheng et al. 2019; Kamal et al. 2019; Miller et al. 2020; Wang et al. 2015).

## 2.8 Surfactant Adsorption, Wettability Alteration, and Imbibition Studies using Biosurfactants

Along with synthetic surfactants, biosurfactants can also be used in conventional reservoirs to increase oil recovery. In carbonates, Saxena et al. 2017 and Madani et al. 2014 showed imbibition of biosurfactants decreases contact angle from 17% to 75%. Adsorption studies by Ahmadi et al. 2013 showed 4 mg-surfactant/gm-rock surfactant adsorption at 28$^{o}$C and 8 wt.% salinity. Another study by Haroon et al. 2017 showed 4.3 mg-surfactant/gm-rock at 50$^{o}$C. Surfactant imbibition studies by Ahmadi et al. 2014 and Ravi et al. 2015 showed 7% to 19.6% additional oil recovery as compared to brine. Gomari et al. 2018 also showed low IFT using biosurfactants (rhamnolipids) because of increased $SO4^{2-}$ ions, as these ions have higher affinity towards carbonates.

Study by Elraies et al. 2010 showed biosurfactants reduce IFT. Nowrouzi et al. 2020 showed imbibition of biosurfactant decreases contact angle in sandstones (53% quartz, 15% feldspars, and 29% iron oxide) from 28% to 88%. Yekeen et al. 2020 also showed a decrease in contact angle using Berea sandstones at 25$^{o}$C and 5 wt.% salinity. Imbibition studies by Ravi et al. 2015; Nowrouzi et al. 2020; Pillai et al. 2020 showed 2% to 32% additional oil recovery using biosurfactants. Okoro et al. 2021 also showed 68.42% residual oil recovery at room temperature using sandstone samples from the Gulf of Guinea.

It is worth mentioning that biosurfactants used in the current literature were synthesized from many sources, such as jatropha oil, coconut oil, palm oil, soybean, soapnut, and mulberry extracts. From the available studies, we can say biosurfactants significantly reduce IFT, alter wettability and thus increase oil recovery in sandstones and carbonates at low salinity and temperature.

Atta et al. 2021 and Camara et al. 2019 showed biosurfactants synthesized from natural oil are stable at high temperature and high saline conditions. Along with being stable, studies by Ines and Dhouha 2015 and Gudina et al. 2015 showed biosurfactants have lower IFT and lower Critical Micellar Concentration (CMC).

From the available studies, it can be seen that the anionic surfactants perform poorly in sandstone reservoirs with high TDS and temperature. Few studies have been done using amphoteric surfactants, and the results look promising, but there are no standardized experimental procedures to evaluate wettability, IFT alteration, imbibition, and adsorption. For biosurfactants, many imbibition studies have shown they lower IFT, alter wettability and increase oil recovery, but most of these studies were performed at low salinity and temperature. No literature is currently available with standardized experimental measurements using plug samples at high temperature and TDS, which shows the effect of salinity and temperature.

This study will test two synthetic surfactants (amphoteric) and one biosurfactant (nonionic) to understand wettability alteration, IFT, surfactant adsorption, and its effect on oil recovery in Bone Spring sandstone formation at high TDS and temperature. This formation was selected as it has been previously identified a potential source of high oil and gas production (Walsh 2006).

# Chapter 3 : Measurement Procedures

This chapter describes experiments performed to measure petrophysical and fluid properties on three sandstone sidewall plug samples, three commercially available surfactants, crude oil, and produced brine from the well site. This chapter also describes the set of correlated experiments performed to understand the interactions between rock samples and surfactant solution to understand which type of surfactants perform better in Bone Spring sandstones with high TDS and temperature. Surfactant solutions were analyzed, and the efficiency of these surfactants in altering wettability, adsorption, and recovering hydrocarbons from sandstone samples was studied.

## 3.1 Petrophysical Analysis

Petrophysical properties such as mineralogy, porosity, and Total Organic Content (TOC) were measured on three sandstone sidewall plug samples for this study.

### 3.1.1 Mineralogy Measurements

Mineralogy of the samples was measured using Fourier Transform Infrared Spectroscopy (Sondergeld & Rai 1993 and Ballard 2007). This technique identifies sixteen different minerals, namely, calcite, dolomite, siderite, pyrite, quartz, aragonite, oligoclase, orthoclase, kaolinite, chlorite, illite, smectite, apatite, mixed-layer clays, albite, and anhydrite by inverting the absorbance spectrum.

Samples are crushed into fine particles and oxidized in a low-temperature plasma asher to remove organic matter. These organic carbon exhibits strong peaks in the mid-infrared region, which overlap absorption peaks of other minerals. The ashed samples are then kept in oven at 100$^{o}$C for at least 4 hours before the measurement. 0.3 gm of potassium bromide (KBr) is made into a 1 mm disc by placing it under vacuum compression. This disc is used as a background measurement. Then 0.0005 gm of sample was measured using a highly sensitive weighing scale,

and 0.3 gm of KBr was mixed vigorously and made into another disc under vacuum compression. Both the background and sample discs are kept inside the Nicolet 6700 FTIR instrument for analysis. A spectroscopy library containing spectra of minerals at different concentrations was used to identify and quantify mineralogy.

### 3.1.2 Porosity Measurements

Total porosity of plug samples was measured by adding gas-filled porosity measured using helium porosimetry and bound-liquid filled porosity measured using a 12MHz GeoSpec Nuclear Magnetic Resonance (NMR) Spectrometer. Before starting the measurement, samples were cleaned by soxhlet extraction using two solvents, first with cyclohexane for 48 hours and then with methanol for 48 hours. After cleaning, the samples were dried in oven at 100 $^{o}$C for 5 to 7 days until their weights stabilized.

### 3.1.3 Total Organic Content Measurements

TOC was measured using the dry pyrolysis technique (Law 1999). Samples were crushed into fine particles (35 mesh). One gm of sample was first acidized with 35% hydrochloric acid to remove carbonates. Then the sample was rinsed with deionized water to remove acid residues and dried in oven at 100 $^{o}$C for 15 minutes. Next, the sample was combusted inside the apparatus to measure TOC by wt.% using a LECO 230 Carbon Analyzer. LECO measures TOC by combustion of organic matter present inside the sample, which generates carbon dioxide, which is converted to TOC by wt.%.

## 3.2 Fluid Characterization

Fluid properties measured in this study were density, Interfacial Tension (IFT), and Critical Micelle Concentration (CMC). Three commercially available surfactants, crude oil, and produced brine from the well site were tested. Surfactant solutions were prepared by mixing surfactants with

produced brine at 2 gallons per thousand gallons (gpt) concertation. First, surfactant stability tests were also performed to check whether the surfactant solutions are stable at 145$^{o}$F (reservoir temperature) and room temperature. Next, TDS and pH of produced brine and surfactant solutions were measured using portable meters, while individual ion species in solution were measured using Inductively Coupled Plasma Spectroscopy (ICP) before and after imbibition experiments by a commercial lab (Soil, Water, and Forage Analytical Lab at the Oklahoma State University).

### 3.2.1 Density Measurements

Produced brine, crude oil, and surfactant solutions density were measured using a Mettler Toledo Densito Handheld density meter at room temperature, reservoir temperature, and atmospheric pressure.

### 3.2.2 Surfactant Stability Tests

Surfactant stability tests were performed on surfactants used in this study to check whether the surfactant solutions are stable at 2 gpt concentration and reservoir temperature. Surfactant solutions were kept in airtight containers under ambient conditions for three days and then inspected for stability. New surfactant solutions were prepared, and the process was repeated at 145 $^{o}$F (reservoir temperature). Stable surfactant solutions should remain transparent, while unstable surfactant solutions should turn translucent (Zeng et al. 2018).

### 3.2.3 Critical Micelle Concentration Measurements

Critical Micelle Concentration (CMC) was measured using DataPhysics DCAT 25 Wilhelmy-Plate Tensiometer under ambient conditions using three surfactant solutions at 2 gpt concentration. Wilhelmy plate method measures surface tension using a force tensiometer based on the Wilhelmy equation (Eq. 4).

$$\sigma = \frac{F_{tens}}{L} = \frac{F_{\perp}}{L * Cos\theta} = \frac{F_G}{L * Cos\theta} \quad (4)$$

where $\sigma$ = surface tension; $F_{tens}$ = tension force to the liquid surface; $L$ = wetted length of Wilhelmy plate; $F_{\perp}$ = tension force acting perpendicularly to the liquid surface; $F_G$ = gravitational force of the formed lamella; $\theta$ = contact angle between the liquid phase and plate

For these measurements, fresh surfactant solutions were prepared by mixing surfactants with produced brine at 2 gpt concentration. The experimental steps are described next:

a) Sample vessel is prepared by rinsing it 2 to 3 times with HPLC-grade water and then drying it in oven for 15 minutes. Wilhelmy plate is prepared by cleaning it under a bunsen burner for 7 to 10 seconds.

b) Syringe, which holds the surfactant solution, and the tube, which brings surfactant from its reservoir to syringe and then from syringe to the sample vessel, are rinsed with multiple purge and refill cycles using HPLC-grade water.

c) Syringe is refilled with surfactant solution and purged for a few seconds to remove water and air from the syringe and tube, which brings surfactant to the sample vessel.

d) DCAT 25 is calibrated with no sample vessel and probe.

e) After successful calibration, sample vessel with 50 gm of HPLC-grade water and a thin stirrer are kept carefully in the DCAT25.

f) Probe holder is locked, and Wilhelmy plate is placed into the holder. Stage with sample vessel is moved upwards until distance between the top of liquid interface and bottom of the Wilhelmy plate is about ~5 mm.

g) Probe is unlocked to start the measurement using CMC software.

h) With the density of surfactant solution, concentration range, number of data points, dosing rate, and duration of stirring after each dosing as the inputs measurement of CMC is started. Dosing rate is the rate at which syringe dispenses a given amount of surfactant into the sample vessel.

i) Wilhelmy plate measures surface tension of HPLC grade water as ~72 mN/m. After that, the syringe starts adding surfactant solution into the vessel, and surface tension measurements are repeated. To measure CMC close to its actual value, it is ensured that the first surface tension reading after addition of surfactant is ~65 mN/m. Also, there are at least 10 data points before the expected CMC value.

### 3.2.4 Interfacial Tension Measurements

Interfacial Tension (IFT) measurements were performed using Drop Shape Analyzer (DSA100E, KRUSS) at ambient conditions between crude oil and three surfactant solutions at 2 gpt concentration along with produced brine. Pendant drop method was used to measure IFT. The experimental steps are described next:

a) Surfactant solutions and produced brine were kept in a quartz cuvette. Cuvette was carefully cleaned and dried to prevent any cross-contamination.

b) Crude oil was slowly dispensed into aqueous solutions through a J-shaped needle facing upwards.

c) Using a high-resolution camera with the density of both fluids as inputs, IFT was calculated by digital processing software using the Laplace equation.

Measurements were repeated 3 to 5 times for surfactant solutions and produced brine to get an average.

### 3.3 Contact Angle Measurements

Contact angle measurements were performed between oil and rock samples with produced brine and three surfactant solutions at 2 gpt concentration under ambient conditions. Drop Shape Analyzer (DSA100E, KRUSS) was used to determine wettability. The equipment uses Sessile drop method to measure contact angle.

Wettability changes by surfactant solutions generally indicate the surfactant's effectiveness at that particular concentration, which helps in selecting the suitable surfactant and concentration. Contact angles ranging from $0^o$ to $75^o$ are water wet, $75^o$ to $105^o$ are intermediate wet, and $105^o$ to $180^o$ are oil wet (Anderson 1986).

The experimental steps are described next:

a) For these measurements, disc was cut from a plug, which was further cut into four fragments.
b) All four fragments were cleaned by soxhlet extraction using two solvents, first with cyclohexane for 48 hours and then with methanol for 48 hours to remove most of the hydrocarbons and water (Zygler et al. 2012).
c) After cleaning, samples were dried in oven at 100 $^o$C for 5 to 7 days until their weights stabilized.
d) After drying, samples were cooled down in a desiccator to bring them down to room temperature.
e) Samples were polished using sandpaper of increasing grit sizes (180, 400, 600, 800, 1200) to create a flat surface.
f) Samples were then saturated in crude oil by imbibing them under vacuum for 24 hrs and then under pressure at 5000 psi for 48 hrs.

g) Contact angles were initially measured by slowly placing a drop of produced brine and surfactant solution at 2 gpt concentration using a syringe needle on the rock surface. Using a high-resolution camera and digital processing software, contact angles were captured as the drop from syringe needle came in contact with the rock surface, and two fluids came into equilibrium (Tiab and Donaldson 2012).

h) Measurements were repeated 5 to 7 times to get an average across the surface of the rock sample. Paper towel was used to absorb excess crude oil from the rock surface.

i) Samples were then imbibed in produced brine and surfactant solutions at 2 gpt concentration, 500 psi, and 145 $^{o}$F.

j) After 24 hours, samples and brine/surfactants were removed and kept in an open jar under ambient conditions to cool them down to room temperature.

k) After 30 to 45 mins, samples were removed, and contact angle measurements were repeated.

### 3.4 Surfactant Adsorption Measurements

Surfactant adsorption measurements were performed on rock samples using three surfactant solutions at 2 gpt concentration using UltraViolet-Visible spectroscopy (Genesys 10S UV-Vis Spectrophotometer, Thermo Scientific). These measurements calculate the amount of surfactant getting adsorbed on the rock sample. UV-Vis spectroscopy uses Lambert-Beer-Lambert law (Eq.5) to calculate absorbance.

$$A = -\log\frac{I_o}{I} = \varepsilon * c * l \tag{5}$$

where $A$ = absorbance (dimensionless); $I_o$= intensity of light passing though reference cell; $I$ = intensity of light passing through sample cell; $\varepsilon$ = molar attenuation coefficient (L/mol*cm); $c$ = molar concentration of solution (mol/L); and $l$ = optical path length (cm).

UV-Vis spectrophotometer produces light at varying wavelengths which is absorbed by surfactant molecules present in the solution. This light is passed through two solutions by keeping them in quartz cuvettes. First: is the reference solution which is produced brine in this case. Second: is the sample solution which is a surfactant solution (produced brine plus surfactant) before it has been exposed to a rock sample. This gives light absorption for surfactant solution. Calibration curves were built to calculate the concentration of surfactant left inside the solution from light absorption. These calibration curves correlate the amount of light absorbed at 0.5, 1, 1.5, and 2 gpt concentrations. Wavelength, which shows the most light absorption, is also identified from these calibration curves. The experimental workflow used for surfactant adsorption measurements is shown in Figure 5.

The experimental steps are described next:

a) Sample was cut from a plug, which was cleaned by soxhlet extraction using two solvents, first with cyclohexane for 48 hours and then with methanol for 48 hours to remove most of the hydrocarbons and water (Zygler et al. 2012).
b) After cleaning, the sample was dried in oven at 100 $^{o}$C for 5 to 7 days until their weights stabilized.
c) After drying, sample was cooled down in desiccator to bring them down to room temperature.
d) Sample was crushed and passed through a sieve to ensure the rock particles were less than 250 μm in size.
e) Rock particles and surfactant solutions at 2 gpt concentration were mixed in a 1:20 weight ratio and were kept in airtight containers in an oven at 145 $^{o}$F.

f) After 24 hours, containers were removed from the oven and were kept under ambient conditions to cool the aqueous solution down to room temperature.

g) Aqueous solutions were transferred from airtight containers to centrifuge tubes. Solutions were centrifuged at 2000 rpm for 10 minutes to separate surfactant solution at the top and rock particles at the bottom.

h) Using a syringe needle, surfactant solutions were collected from the centrifuge tubes and were transferred to quartz cuvettes by passing them through a 0.20 μm syringe filter to remove any leftover rock particles.

i) UV-Vis spectroscopy measurements were performed using produced brine in the reference cell and surfactant solutions in the sample cell to get light adsorption.

j) Calibration curves were used to calculate the surfactant concentration of remaining solution and then calculate the amount of surfactant adsorbed on the rock sample using Eq. 6 (Alvarez et al. 2017).

$$\theta_A = \frac{\left(\emptyset_{surf}^{i} - \emptyset_{surf}^{f}\right) * V_{surf} * \rho_{surf} * 10^5}{w_{rock}} \tag{6}$$

where $\theta_A$ = amount of surfactant adsorbed on rock sample (mg of surfactant/gm of rock); $\emptyset_{surf}^{i}$ = initial surfactant concentration (gpt); $\emptyset_{surf}^{f}$ = final surfactant concentration (gpt); $V_{surf}$ = volume of surfactant solution (ml); $\rho_{surf}$ = density of surfactant solution (gm/cc); and $w_{rock}$ = weight of a rock (gm).

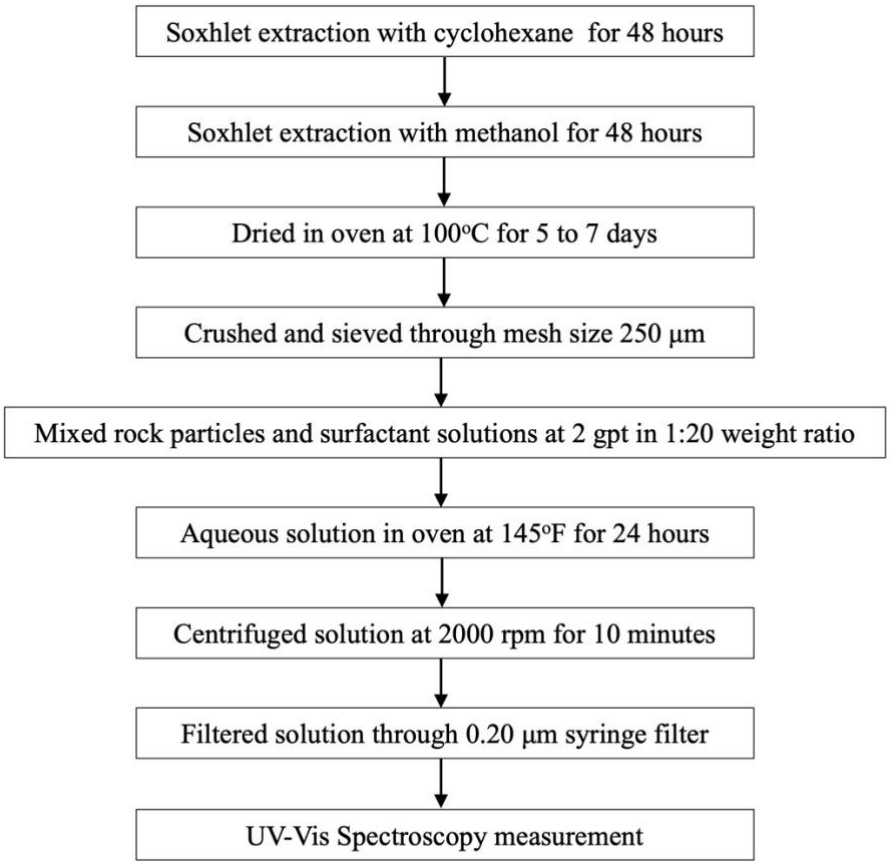



**Figure 5 - Step by step experimental workflow for surfactant adsorption measurements used in this study.**

### 3.5 Imbibition Experiments using Produced Brine and Surfactants

Imbibition experiments were performed on three plug samples using produced brine and three surfactant solutions at 2 gpt concentration, 500 psi, and 145°F to quantify the oil recovery using a 12 MHz NMR Spectrometer. The experimental setup and workflow are shown in Figure 6 and Figure 7.

The experimental steps are described next:

a) Plug samples of 1-inch diameter and 1 to 1.3-inch thickness were cleaned by soxhlet extraction using two solvents, first with cyclohexane for 48 hours and then with methanol for 48 hours, to remove most of the residual hydrocarbons and water (Zygler et al. 2012).

b) After cleaning, the samples were dried in an oven at 100 $^{o}$C for 5 to 7 days until their weights stabilized.

c) After drying, samples were cooled down in desiccator to bring them down to room temperature.

d) NMR T2 and T1-T2 were measured to calculate the volume of bound fluid left inside the sample.

e) Samples were then imbibed in crude oil under vacuum for 24 hrs and then under pressure at 5000 psi for 48 hrs to saturate them with oil. A high-pressure vessel connected to hydraulic hand pump with pressure gauge was used for the pressure saturation process. Crude oil and samples were kept inside the pressure vessel, and the fluid pressure was applied using dodecane. To avoid contamination, samples with crude oil were separated from dodecane using a sealed piston.

f) NMR T2 and T1-T2 were again measured to calculate the sample's total fluid volume (bound fluid plus oil).

g) Samples were then imbibed in produced brine at 500 psi and 145 $^{o}$F for 24 hours. A high-pressure vessel connected to a pump (Varian SD-1 Prep Star Solvent Delivery Module) with pressure gauge was used for the imbibition process. Sample was kept inside the pressure vessel with brine, and the fluid pressure was applied by adding more brine, ensuring no airflow. As the pressure reached 500 psi, valve connecting the pump and pressure vessel was closed. Pressure inside the vessel was monitored using the pressure gauge. Heating tape connected to a rheostat (Variac Transformer Variable AC Voltage Regulator) was wrapped around the pressure vessel to make brine present inside the vessel reach reservoir temperature.

h) After 24 hours, samples and produced brine were removed. Samples were kept imbibed in the same brine in an open jar to cool the samples down to room temperature.

i) NMR T2 and T1-T2 were again measured to calculate the volume of oil left inside the sample after imbibition. Figure 8 shows NMR T1-T2 after drying, oil saturation, and after imbibition (post-recovery). Oil recovery was calculated using Eq. 7

$$Oil\ Recovery\ (\%) = \frac{Initial\ Volume\ of\ Oil\ (ml) - Final\ Volume\ of\ Oil\ (ml)}{Initial\ Volume\ of\ Oil\ (ml)} * 100 \qquad (7)$$

where Initial Volume of Oil (ml) = Total Volume of Fluid inside Sample after Oil Saturation (ml) – Volume of Bound Fluid inside Sample after Drying (ml)

This procedure was repeated, and oil recovery was calculated using surfactant 1. Before going to surfactant 2, using the same procedure, oil recovery was again calculated using produced brine to see that the sample reached the same baseline and there was no alteration in samples from surfactant 1 imbibition. Series of imbibition tests repeated on the same three samples in order of testing using produced brine and three surfactants are shown in Table 1. Also, NMR T2 was measured after each oil saturation to ensure that the samples reached similar oil saturation before each recovery measurement, as shown in Figure 9.

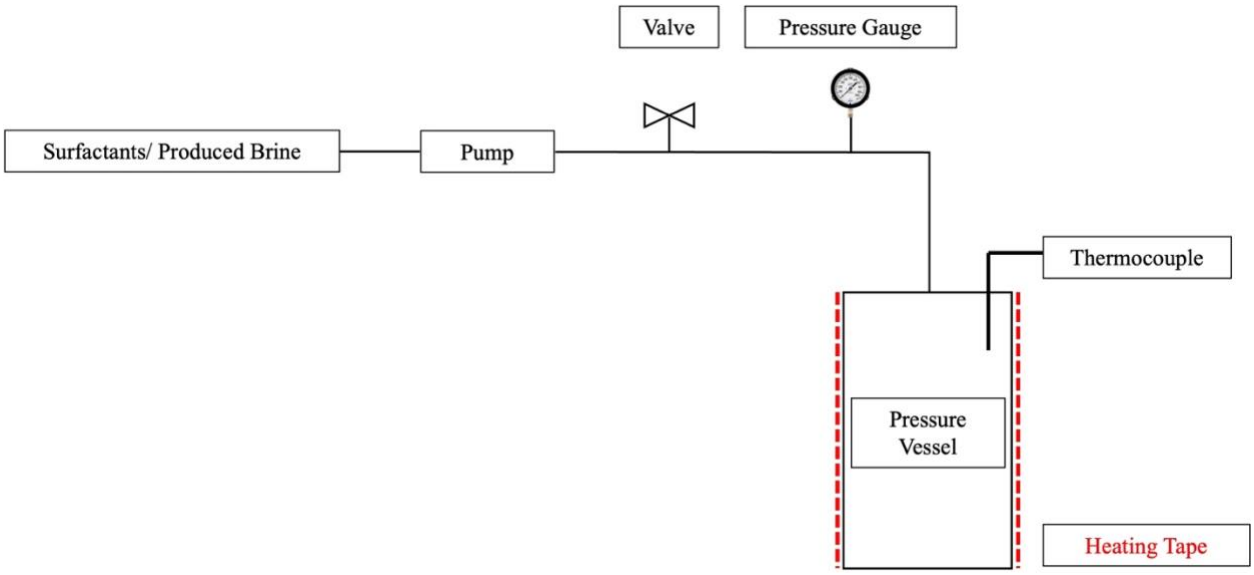



**Figure 6 - Experimental setup used in this study to imbibe plug samples in produced brine and surfactant solutions.**

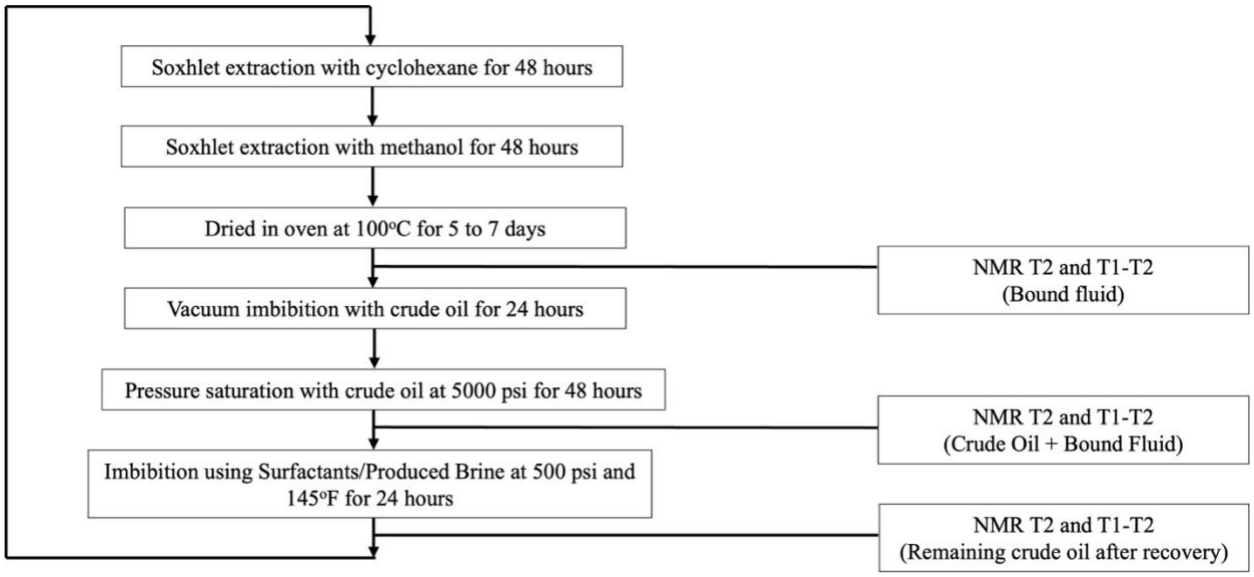



**Figure 7 - Step by step experimental workflow for produced brine and surfactant imbibition measurements used in this study.**

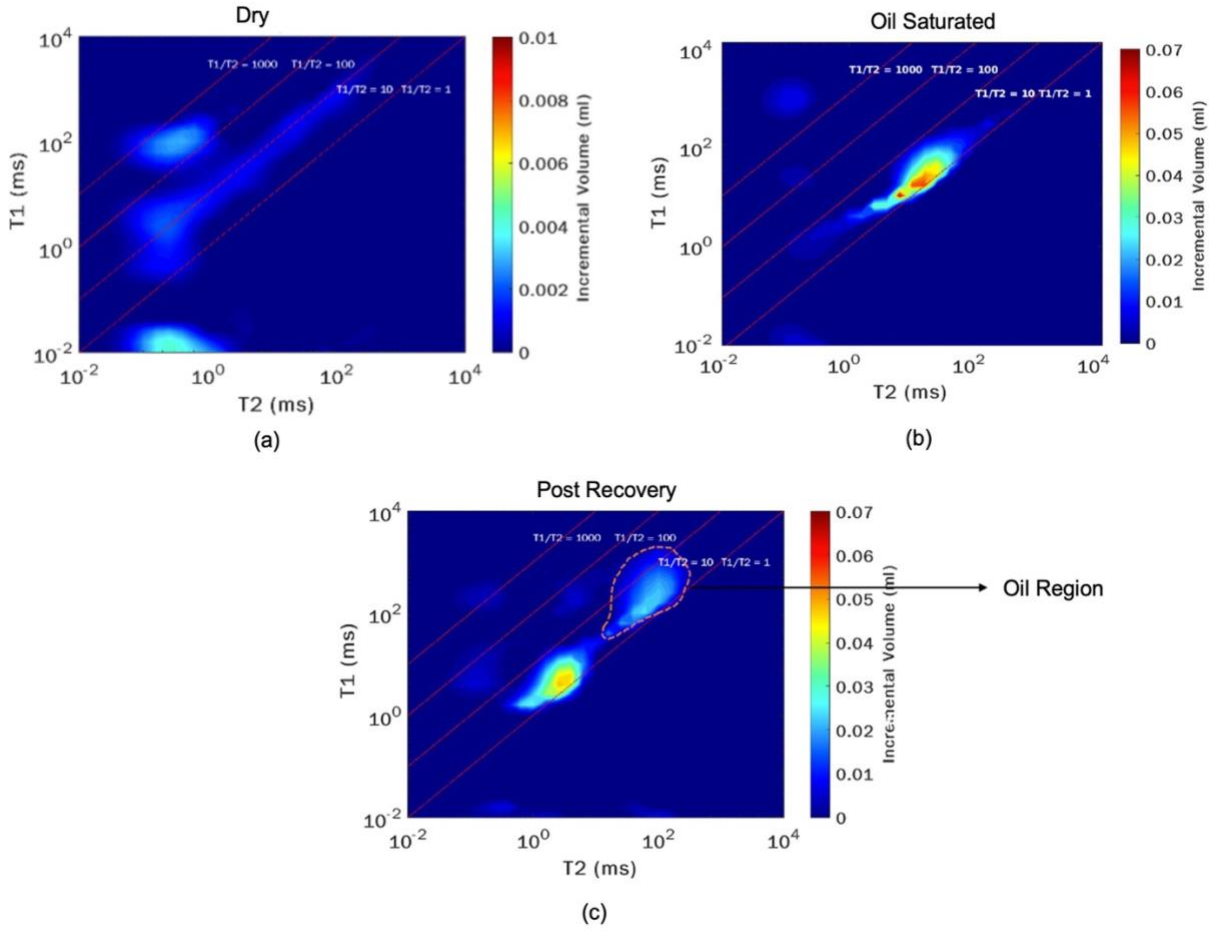



**Figure 8 - NMR T1-T2 maps of sandstone samples pre and post-imbibition using produced brine. (a) shows bound fluid inside the sample after cleaning and drying, (b) shows the total volume of total fluid inside the sample (crude oil plus bound fluid) after oil saturation with one signal relaxing elongated over T1/T2 ratio due to presence of hydrocarbons with varying carbon number, and (c) showing two main signals relaxing at different T1/T2 ratios which indicate presence of two different fluids inside the sample. Highlighted region here shows oil present inside the sample post-imbibition.**

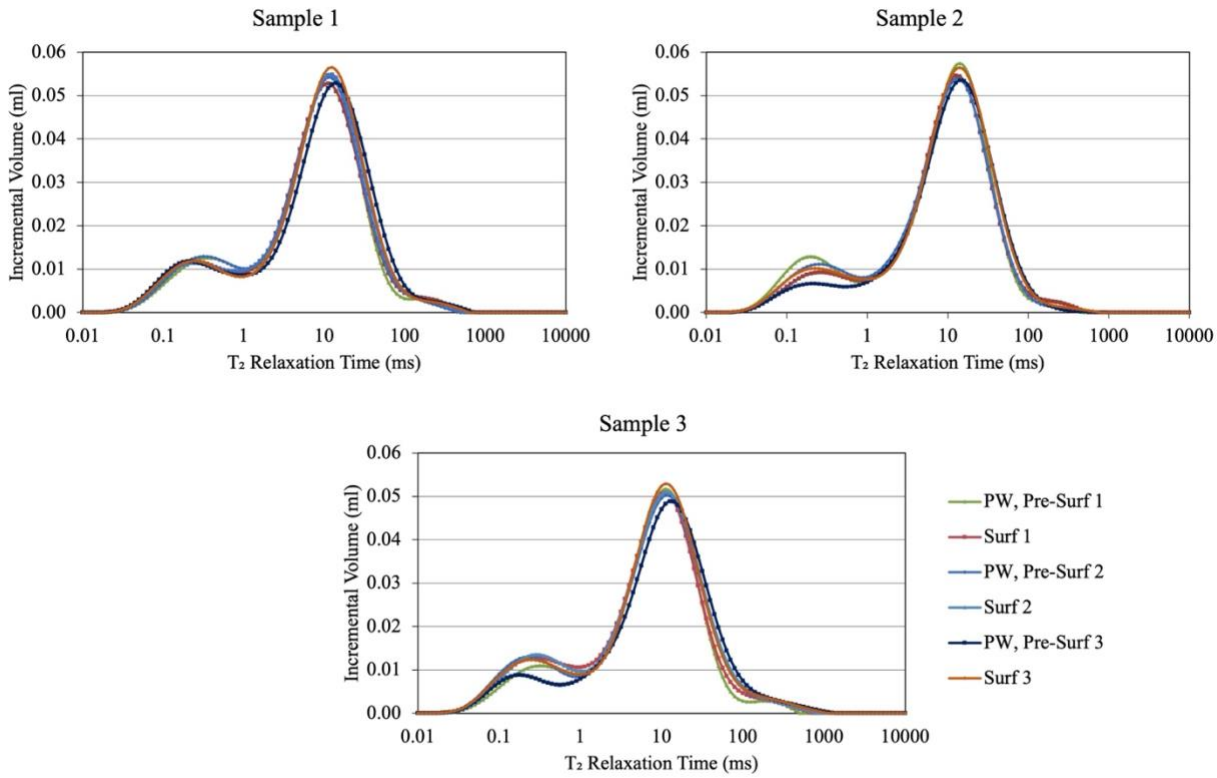



**Figure 9 - NMR T2 measurements of three samples saturated with oil before imbibition. T2 spectra here show two peaks, with second peak having higher amplitude showing oil inside the sample. With all the T2 spectra overlapping each other very closely, we can say that the sample reached similar initial oil saturation.**

| Order of Testing | Description |
|---|---|
| 1 | Produced Brine, Pre-Surfactant 1 |
| 2 | Surfactant 1 |
| 3 | Produced Brine, Pre-Surfactant 2 |
| 4 | Surfactant 2 |
| 5 | Produced Brine, Pre-Surfactant 3 |
| 6 | Surfactant 3 |

**Table 1 - Test matrix showing imbibition measurements performed on same three samples in testing order to quantify the oil recovery.**

### 3.6 Determination of Water and Oil Region in NMR T1-T2 Maps

After imbibition with produced water and surfactants, we see two regions in NMR T1-T2 maps, as seen in Figure 10. We know the two regions represent water and oil present inside the sample due to the viscosity difference between the two fluids, but we are not aware of which region is water and which region is oil. To distinguish these regions in NMR T1-T2 maps and to calculate the final volume of oil left inside the sample after imbibition, samples were imbibed in $D_2O$ (NMR doping agent).

Samples were imbibed in a $D_2O$ solution with 237,705 TDS at room temperature to allow diffusion of $D_2O$ into the sample and $H_2O$ out of the sample. $D_2O$ solution equal to the TDS of produced brine was used to eliminate the effect of TDS in diffusion process. $D_2O$-$H_2O$ diffusion was monitored for 8 days using NMR T2 and T1-T2 measurements, as shown in Figure 11. $D_2O$ is an isotope of water, with each deuterium atom having one neutron. It is perfectly miscible with water and immiscible with oil. After diffusion of $D_2O$ into the sample, water can be detected by a decrease in the NMR signal while the oil signal remains constant (Gannaway 2014).

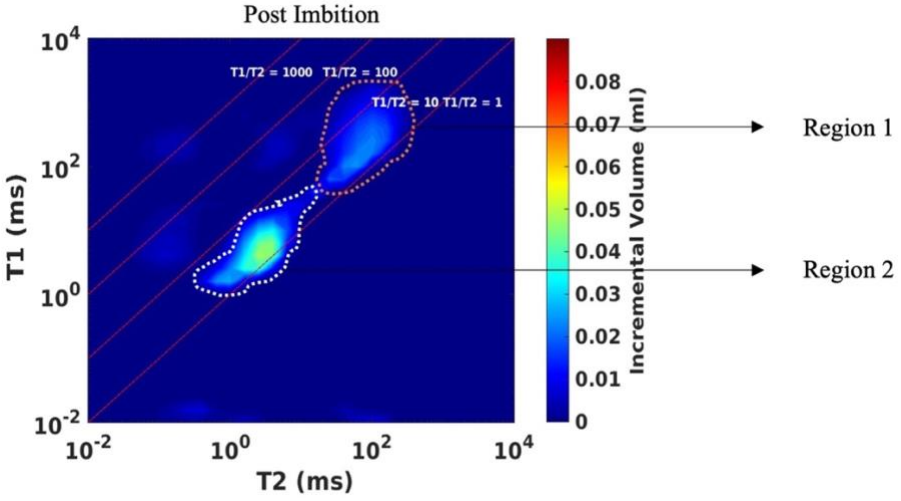



**Figure 10 - NMR T1-T2 map showing two signals relaxing at different T1/T2 ratios after imbibition with produced brine, pre-surfactant 1.**

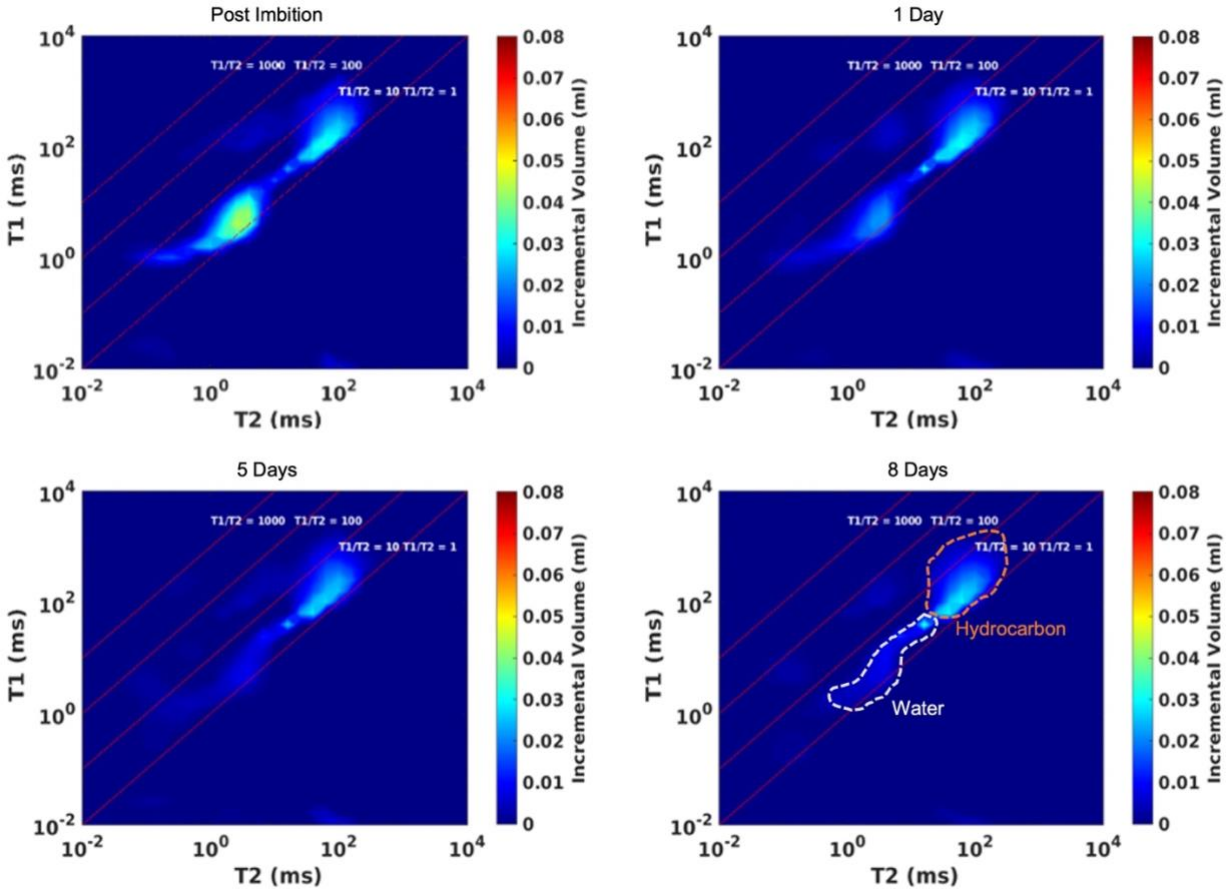



**Figure 11 - NMR T1-T2 maps of sandstone sample after imbibition with NMR doping agent. Post imbibition with brine, sample shows two signals relaxing at different T1/T2 ratios. To distinguish water and oil signal and to quantify oil recovery, sample was imbibed in $D_2O$ for 8 days. With time we see a decrease in amplitude of signal having faster relaxation, which shows it is water, while the signal having slower relaxation remains the same, which shows it is oil.**

# Chapter 4 : Results and Discussion

## 4.1 Petrophysical Analysis

Table 2 shows the petrophysical properties of three plug samples used in this study for imbibition experiments. Samples were rich in quartz (41 to 52 wt.%) and clays (29 to 34 wt.%), along with the presence of carbonates and feldspars. Samples also have helium porosity of 17 to 19% and very low TOC of 0.4 to 0.8 wt.%

Additionally, five more plugs were used in this study in this study to analyze relationship between surfactant adsorption and mineralogy (Table 3). These samples have clay (11 to 50 wt.%), quartz (28 to 60 wt.%), along with the presence of carbonates and feldspars.

| Sample | Quartz (wt.%) | Clays (wt.%) | Carbonates (wt.%) | Feldspars (wt.%) | TOC (wt.%) | Helium Porosity (%) | Total Porosity (%) |
|---|---|---|---|---|---|---|---|
| Sample 1 | 52 | 29 | 8 | 5 | 0.53 | 17.9 | 19.6 |
| Sample 2 | 49 | 30 | 11 | 7 | 0.48 | 17.8 | 19.9 |
| Sample 3 | 41 | 34 | 9 | 12 | 0.54 | 19.1 | 20.9 |

**Table 2 - Mineralogy, TOC, and porosity of Bone Spring sandstone samples used in this study for imbibition experiments.**

| Sample | Quartz (wt.%) | Clays (wt.%) | Carbonates (wt.%) | Feldspars (wt.%) |
|---|---|---|---|---|
| BS 1 | 60 | 11 | 6 | 23 |
| BS 2 | 60 | 21 | 0 | 18 |
| BS 3 | 48 | 27 | 2 | 13 |
| BS 4 | 51 | 35 | 8 | 5 |
| BS 5 | 28 | 50 | 5 | 5 |

**Table 3 - Mineralogy of Bone Spring sandstone samples used in this study to analyze relationship between surfactant adsorption and mineralogy.**

### 4.2 Fluid Characterization

#### 4.2.1 Density Measurements

Three commercially available surfactants were tested at 2 gpt concertation along with produced brine. Surfactants description is given in Table 4. These surfactants were explicitly designed to be stable in reservoirs with high TDS and high temperature with low IFT to increase oil recovery. Density of produced brine, crude oil, and surfactant solutions at 2 gpt concentration are summarized in Table 5.

| Surfactant Name | Surfactant Type | Key Components | Concentration (wt %) |
|---|---|---|---|
| Surfactant 1 | Amphoteric | Ethylene Glycol | 5 – 10 |
| | | Glycerol | 1 – 5 |
| | | Sodium Chloride | 1 – 5 |
| | | Proprietary Oxyalkylated alcohol | 1 – 5 |
| | | Proprietary Alkyl Sultaine | 5 – 10 |
| | | Proprietary Organic Sulfonic Acid | 1 – 5 |
| Surfactant 2 | Amphoteric | Proprietary Alkyl Sultaine | 10 – 30 |
| | | Ethylene Glycol | 10 – 30 |
| | | Sodium Chloride | 1 – 5 |
| Surfactant 3 | Nonionic Biosurfactant | Glycolipids | 25 – 75 |

**Table 4 - Description of different surfactants used in this study.**

| Fluid Name | Density (g/cc) |
|---|---|
| Crude Oil | 0.780 |
| Produced Brine | 1.130 |
| Surfactant 1 | 1.131 |
| Surfactant 2 | 1.132 |
| Surfactant 3 | 1.138 |

**Table 5 - Density of crude oil at 145ºF along with produced brine, and surfactant solutions at 2 gpt concentration and 70ºF.**

### 4.2.2 Surfactant Stability Tests

Results from surfactant stability tests performed on three surfactant solutions prepared by mixing surfactants with produced brine at 2 gpt concentration shows that surfactants are stable as the solution remained transparent after 3 days at ambient condition (70ºF) and reservoir temperature (145ºF). Figure 12 shows the transparent solutions for three surfactants at 2 gpt concertation, with a blank sample having brine.

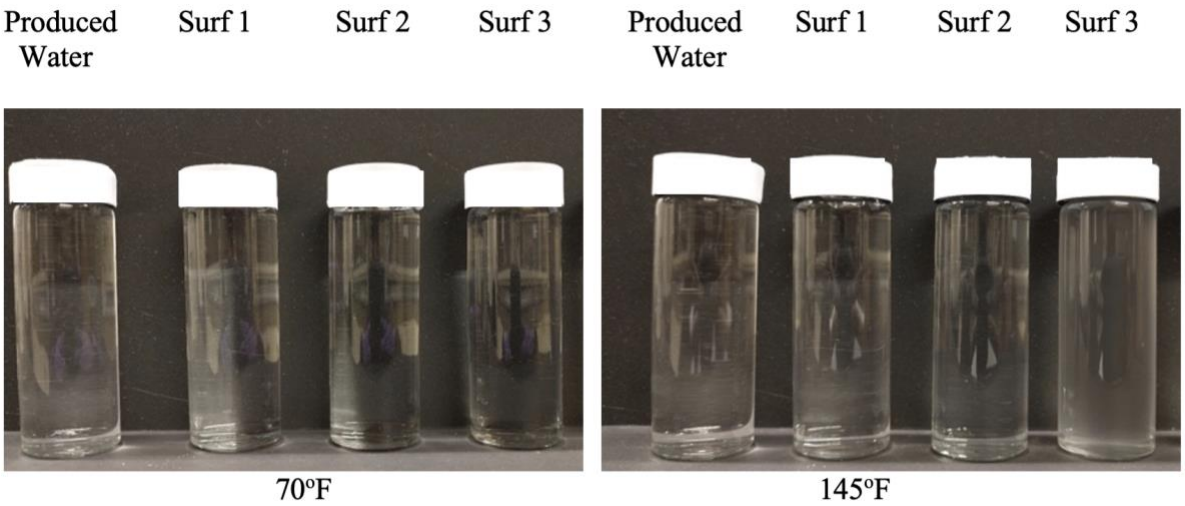



**Figure 12 - Surfactant stability tests shows surfactants are stable at 2 gpt concentration as the solutions remained transparent after 3 days at 70ºF and 145ºF.**

### 4.2.3 pH Measurements

pH measurement results of produced brine and surfactant solutions are shown in Figure 13. Results show that produced brine has neutral pH, and even after adding surfactants at 2 gpt concentration, the solution pH still remains neutral. This is important as pH of the solution affects net charge on the clay surface and charge on the hydrophilic head of amphoteric surfactant. Since the surfactant solution is neutral, for this study, we assume that sandstone have a negative surface charge due to clay minerals (Lee et al. 2019).

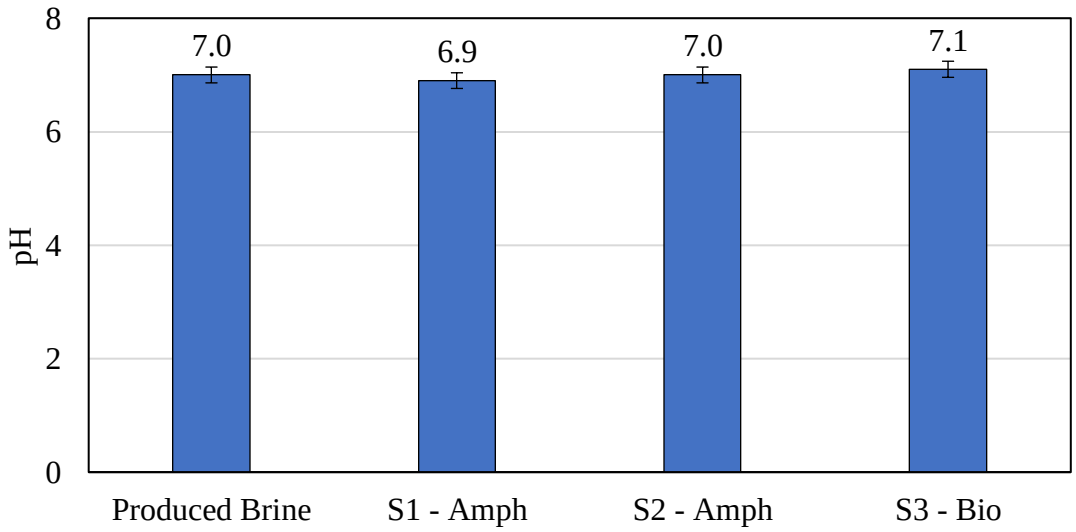



**Figure 13 - IFT measurement of produced brine and three surfactants at 2 gpt concentration.**

### 4.2.4 ICP Analysis: Before Imbibition Experiments

Major constituents of produced brine and surfactant solutions measured using ICP analysis are shown in Figure 14. Table 6 summarizes the ion analysis of produced brine with TDS of 237,705 ppm.

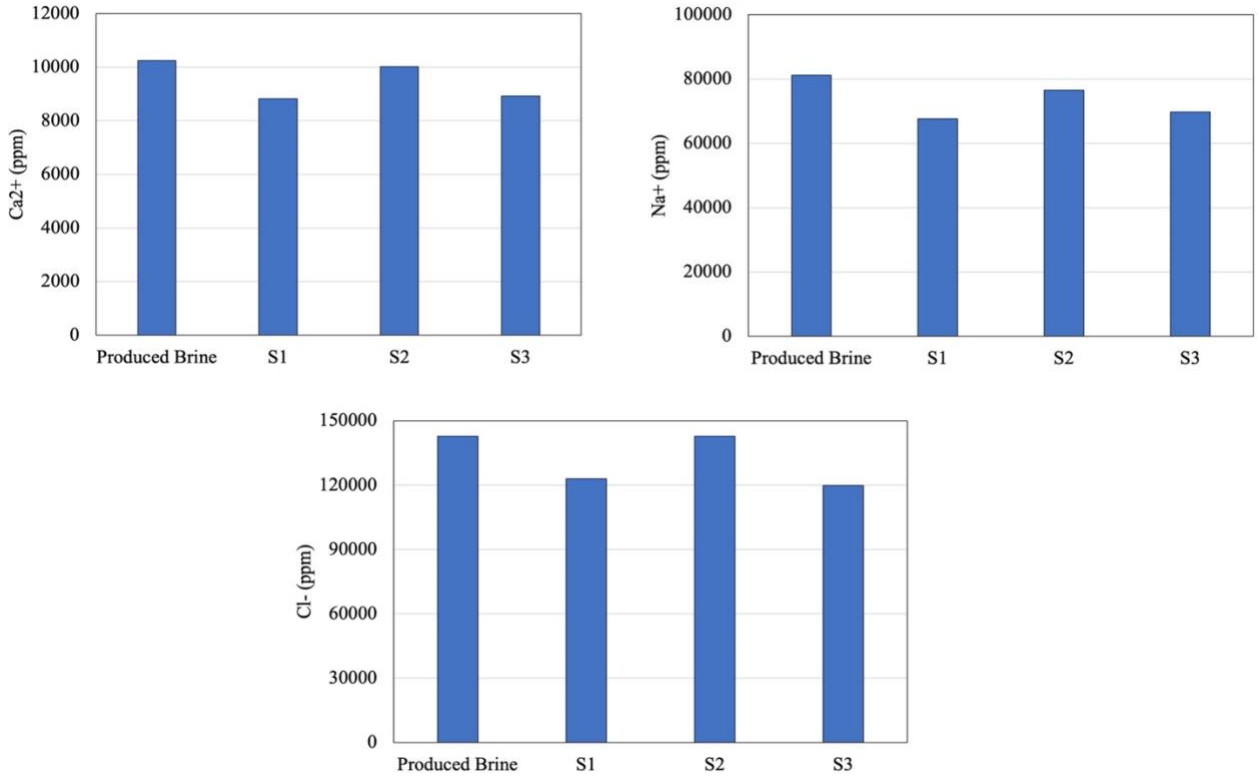



**Figure 14 - ICP analysis of produced brine and surfactant solution at 2 gpt concentration showing major ion constituents.**

| Ion | Concentration (ppm) |
|---|---|
| $Na^+$ | 81210 |
| $K^+$ | 1664 |
| $Ca^{2+}$ | 10251 |
| $Mg^{2+}$ | 1478 |
| $Cl^-$ | 142826 |
| $SO_4^{2-}$ | 206 |
| $HCO_3$ | 70 |
| TDS | 237,705 |

**Table 6 - Ion analysis of produced brine.**

### 4.2.3 Critical Micelle Concentration Measurements

Surface tension at variable concentrations for CMC measurement under ambient conditions are shown in Figure 15. CMC measurements in Table 7 shows that at 2 gpt concentration, we are higher than the CMC, and surfactant solutions should show a maximum reduction in IFT.

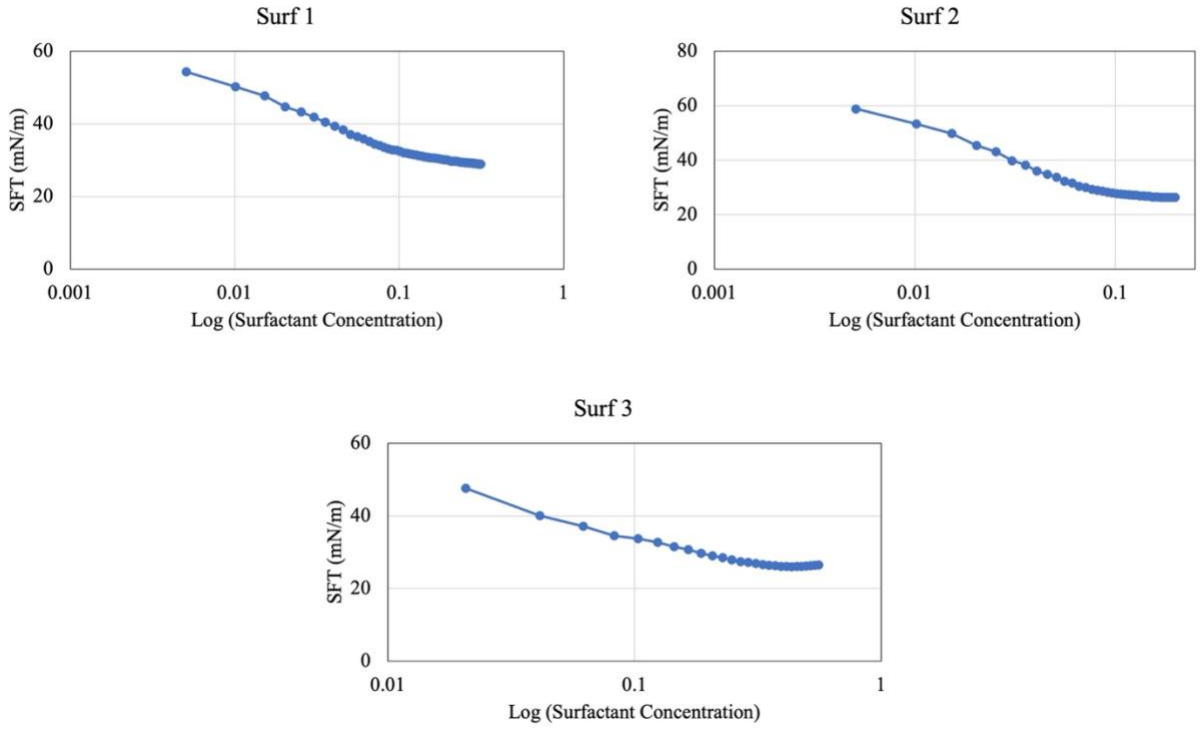



**Figure 15 - Surface tension at variable surfactant concentration for CMC measurement.**

| Fluid Name | CMC (gpt) |
|---|---|
| Surfactant 1 | 0.12 |
| Surfactant 2 | 0.04 |
| Surfactant 3 | 0.26 |

**Table 7 - CMC measurements of surfactants used in this study.**

### 4.2.4 Interfacial Tension Measurements

Results from fluid/fluid interactions between crude oil and surfactants at 2 gpt concentration, along with produced brine, are shown in Figure 16. The original IFT between crude oil and brine was 17.3 mN/m. Then as surfactants were added to the brine, IFT was reduced moderately to 3.6 and 4.4 mN/m for amphoteric surfactants, while biosurfactant showed the most reduction in IFT to 0.7 mN/m. With CMC values lower than 2 gpt concentration, we can say this is the maximum reduction in IFT possible using these surfactants at such a high TDS.

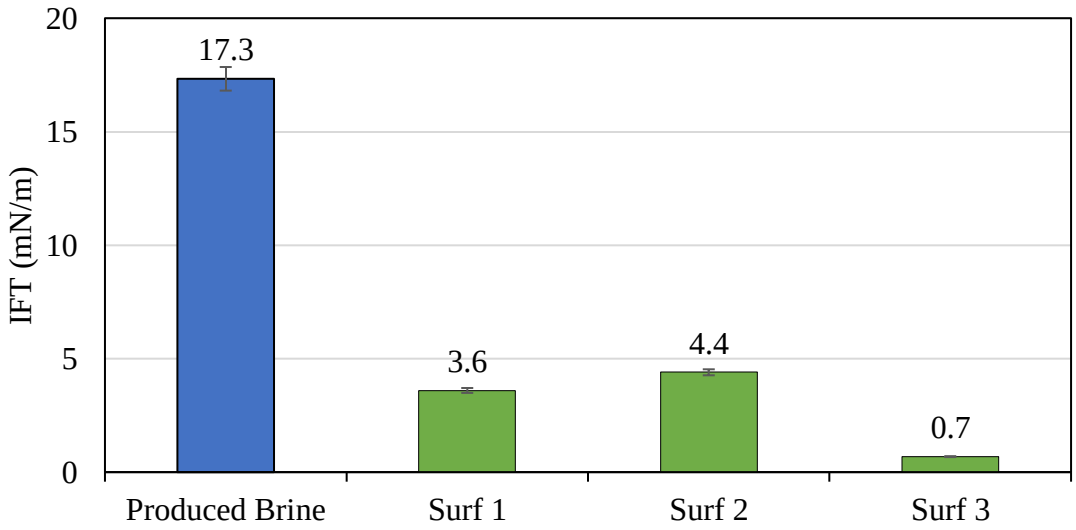



**Figure 16 - IFT measurement of produced brine and surfactants at 2 gpt concentration.**

### 4.3 Contact Angle Measurements

Results from contact angle measurements between rock samples and surfactants at 2 gpt concentration, along with produced brine, are shown in Figure 17. Base case wettability measurement after saturation with crude oil shows that the rock samples are oil-and-intermediate wet with contact angles ranging from 92 to 110 degrees. After determining initial wettability, rock samples were imbibed with produced brine and surfactants at 2 gpt concentration. Measurements post imbibition shows that with produced brine, the contact angle remains approximately 94

degrees which shows that the sample is still intermediate wet. All the surfactants reduced contact angle and made the samples water wet, but biosurfactant was the most effective.

Basic crude oil components get strongly adsorbed on sandstone samples as they have negatively charged surface active agents (Doust et al., 2011). Initially, this made all the samples oil-and-intermediate wet. Amphoteric surfactants with neutral pH behave as zwitterionic with both positive and negative charges on the hydrophilic head (Schramm 2000; Lake 1989; Honciuc 2021). Current measurements indicate that a negative charge on the head of amphoteric surfactants interacts with positively charged oil molecules (basic component of the adsorbed oil) and form an ion-pair, as shown in Figure 18. This leads to desorption of oil from the rock surface, which makes the sample water wet (Standnes & Austad 2000).

Nonionic biosurfactants have a hydrophilic head with overall no charge. There are no electrostatic interactions between the surfactant and rock surface for biosurfactant, but it still makes the sample most water wet.

Here I hypothesize that with produced brine having high TDS, precipitation of divalent cations such as $Ca^{2+}$ takes place on clay surface, as shown by Liu et al. 2019 in Figure 19. This precipitation is higher in amphoteric surfactants as compared to biosurfactants which decreases the efficacy of amphoteric surfactants to decrease contact angle.

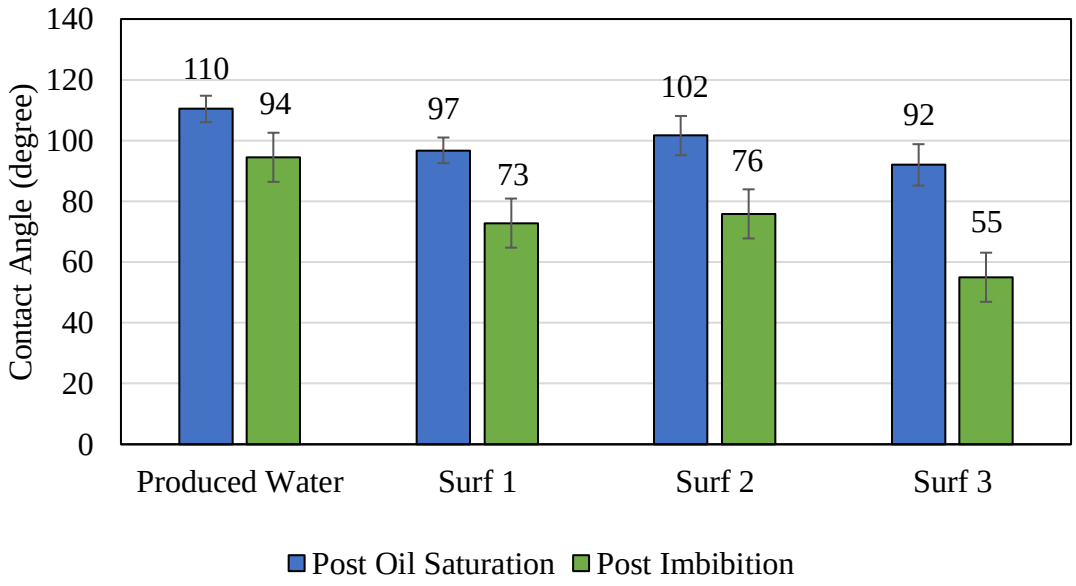



**Figure 17 - Contact angle measurements between sandstone samples and surfactants at 2 gpt concentration along with produced brine used in this study. Measurements post oil saturation shows all the samples are oil-and-intermediate wet. After imbibition with brine, the sample remains intermediate wet. With surfactants, the samples become water wet.**

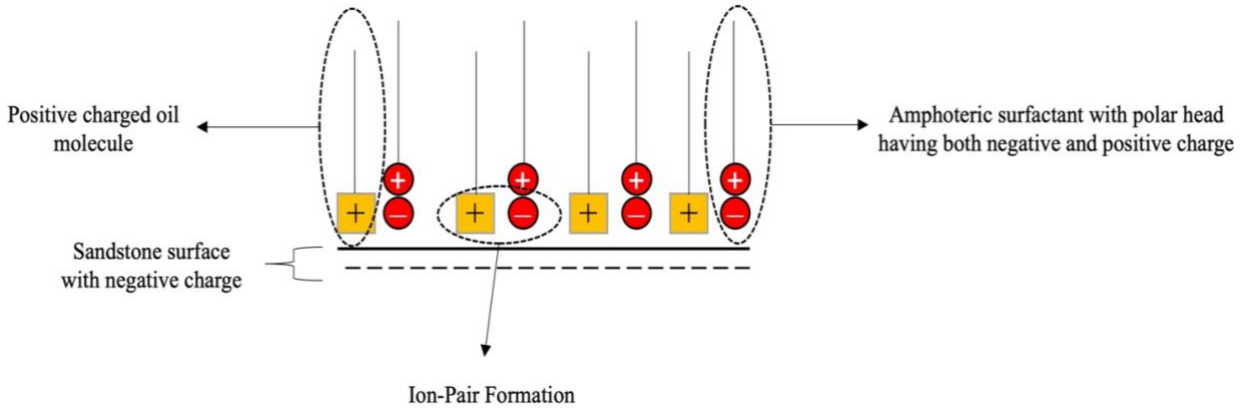



**Figure 18 - Model showing ion-pair formation using oil-wet sandstone samples.**

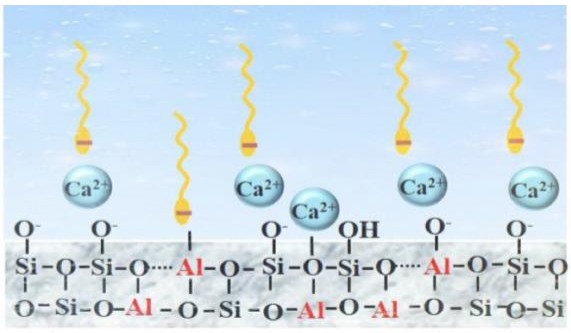



**Figure 19 - Schematic illustration of the adsorption mechanism at water-clay interface (Liu et al. 2019).**

### 4.4 Surfactant Adsorption Measurements

Surfactant adsorption measurements were performed to calculate the amount of surfactant adsorbed on the rock surface. Using Eq. 7 with an initial surfactant concentration at 2 gpt, final surfactant concentrations were measured in the solutions using UV-Vis spectrophotometer. For this measurement, calibration curves were built. Figure 20 shows the light absorption spectrum for three surfactants at concentrations varying from 0.5, 1, 1.5, and 2 gpt. Solutions with increasing surfactant concentration showed increasing light absorption with a peak at a particular wavelength. Light absorption was recorded at absorption peak wavelength of 240 nm for all three surfactants to build calibration curves, as shown in Figure 21. Final surfactant concentrations were calculated using these calibration curves by measuring light absorption on surfactant solution post imbibition. Light absorption spectrum post imbibition are shown in Figure 22, and surfactant adsorption results are shown in Figure 23.

Results from surfactant adsorption measurements showed that amphoteric surfactants have higher surfactant adsorption of 15 and 17 mg/gm-rock, while biosurfactant have least surfactant adsorption of 9 mg/gm-rock. Surfactant adsorption depends on the reactivity between the surfactant solution charge and the rock surface charge. Due to neutral pH of surfactant solution, clay minerals are negatively charged. Here I hypothesize that the positive charged polar head of

amphoteric surfactant and negative charge clay surface are attracted to each other because of electrostatic forces of attraction and form an ion-pair, as shown in Figure 24. With produced brine having high TDS, precipitation of divalent cations such as $Ca^{2+}$ occurs on clay surface. Liu et al. 2019 showed that in mixed cation solutions such as produced brine with both $Na^{+}$ and $Ca^{2+}$, clay surfaces prefer adsorption of $Ca^{2+}$. These divalent cations on clay surface acts as cationic bridge between the negative charged polar head of amphoteric surfactant and negative charge on clay surface, which originally should have electrostatically repelled each other because of same charge as showed by Liu et al. 2021 as shown in Figure 25.

Higher concentration of $Ca^{2+}$ in surfactant solution, higher are the cationic bridges which increases surfactant adsorption on clay minerals and form a multilayer of adsorped surfactants, as shown in Figure 26. Atta et al. 2020 and Gupta and Mohanty, 2008 also showed that surfactant accumulation from bulk solution to the sandstone surface occurs in surfactant solutions with high TDS. Liu et al. 2019 also showed that a decrease in salinity decreases surfactant adsorption. The main reason for decline in adsorption was a decrease in divalent cations due to reduction in salinity.

Here I also hypothesize that these divalent cations, as shown in Figure 27 also reduce electrostatic repulsion between the same charge on polar head of surfactants present over clay surface, further increasing surfactant adsorption.

With biosurfactant having no overall charge, there are no electrostatic interactions between the charges in surfactant solution and rock surface. Such surfactants get dissolved into brine and then adsorped onto the rock surface by hydrogen bonding and van der Waals interactions, as shown previously by Nowrouzi et al. 2021 and Paternina et al. 2020. These forces are weaker compared to electrostatic attraction, leading to much lower biosurfactant adsorption.

In conclusion, results indicate that using biosurfactants at high TDS and temperature, surfactant adsorption from bulk solution to sandstone surface is lower as compared to amphoteric surfactants. High adsorption of amphoteric surfactants is due to presence of divalent cations, which get adsorbed on the clay surface. Here I hypothesize that presence of clays is the main reason for adsorption in these sandstone plug samples at high TDS and temperature.

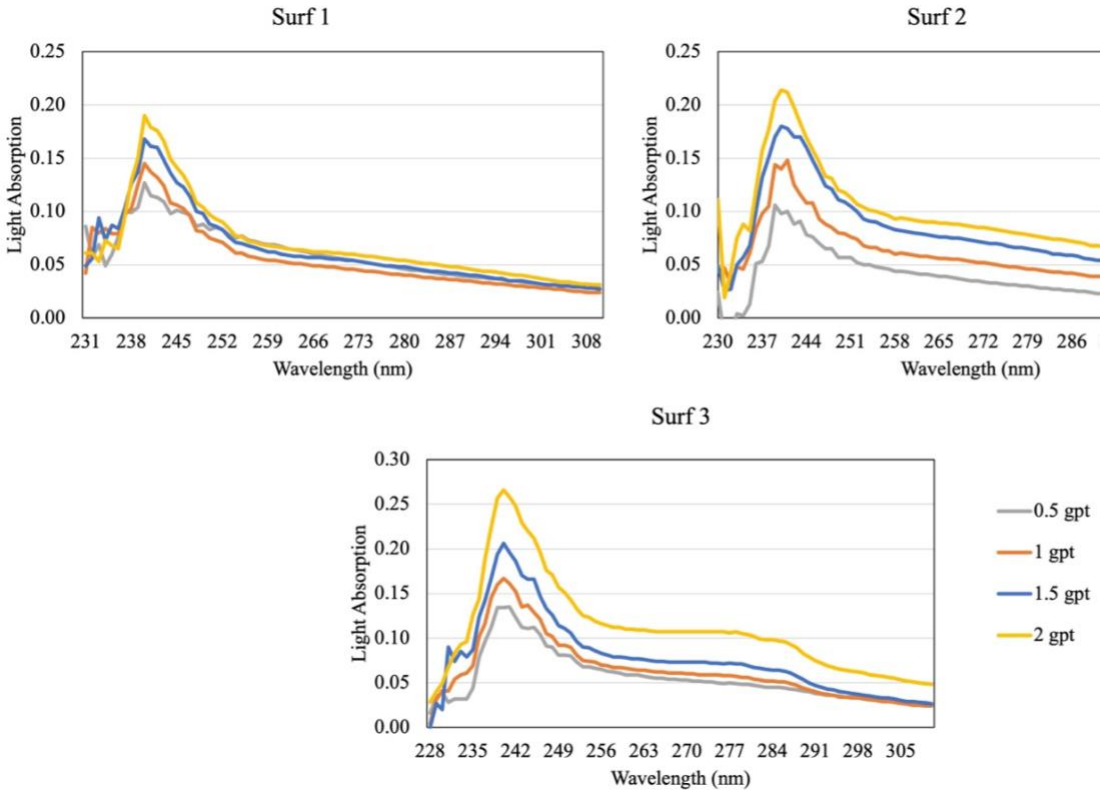



**Figure 20 - Light absorption spectrum for surfactant solutions measured at varying concentrations using UV-Vis spectrophotometer.**

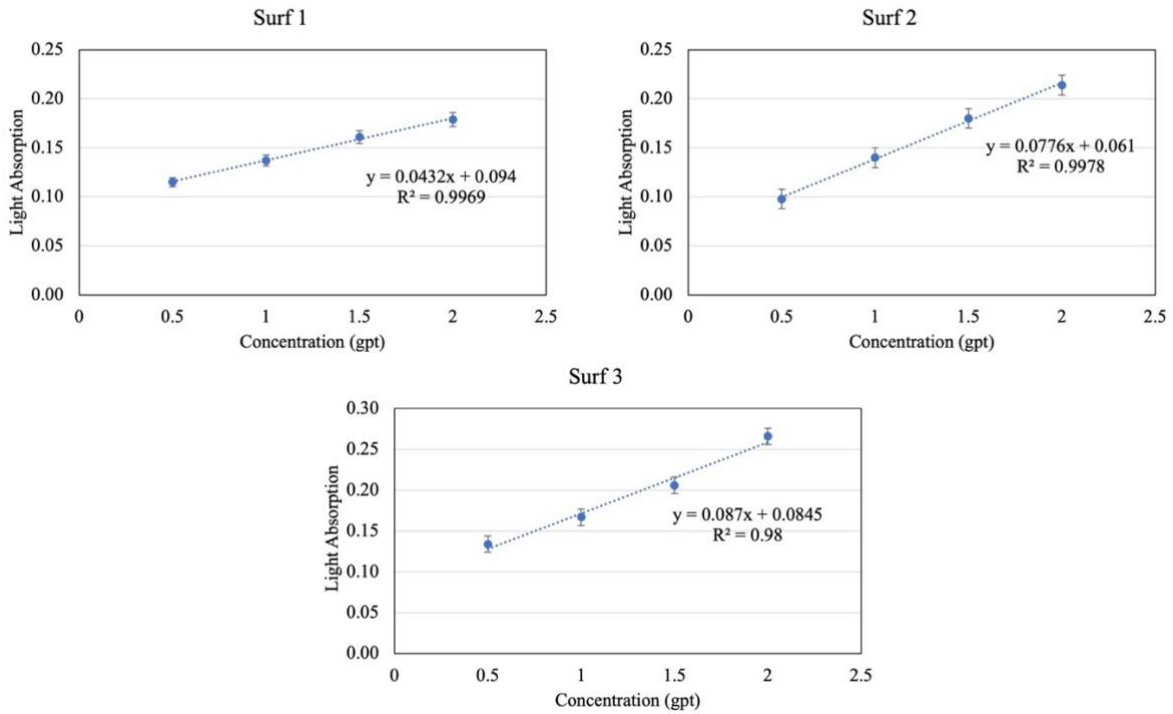



**Figure 21 - Calibration curves for surfactants used in this study. Here recorded light absorptions were plotted at peak absorption wavelength of 240 nm at varying surfactant concentrations for three surfactants.**

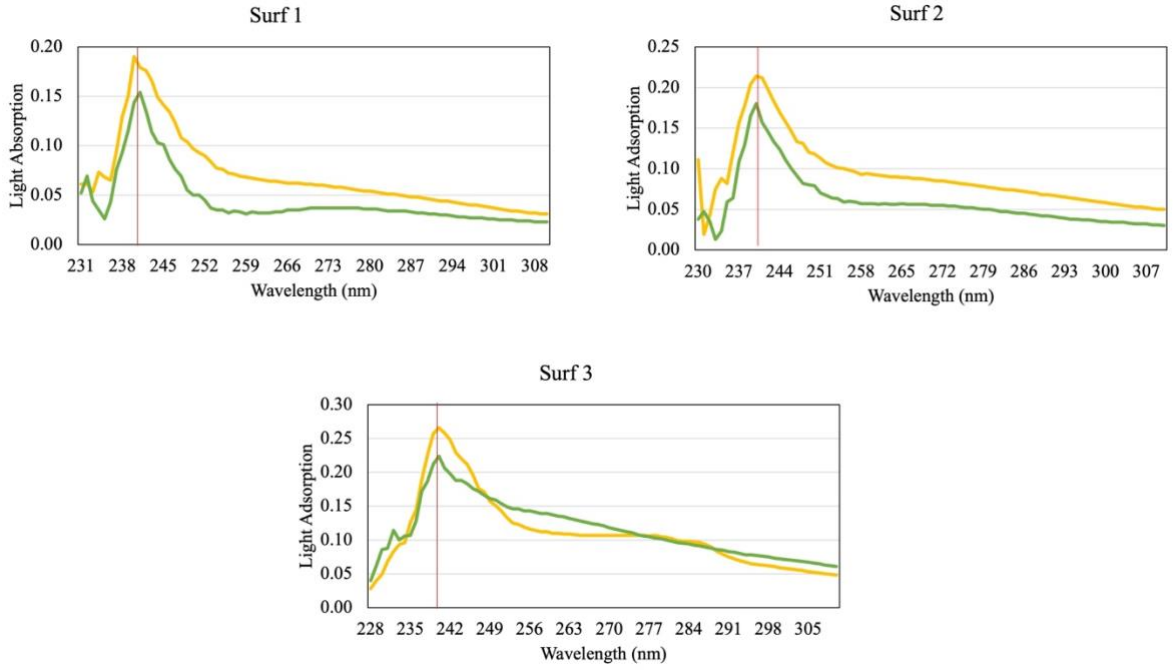



**Figure 22 - Light absorption spectrum for surfactant solutions post imbibition at 2 gpt concentration using UV-Vis spectrophotometer.**

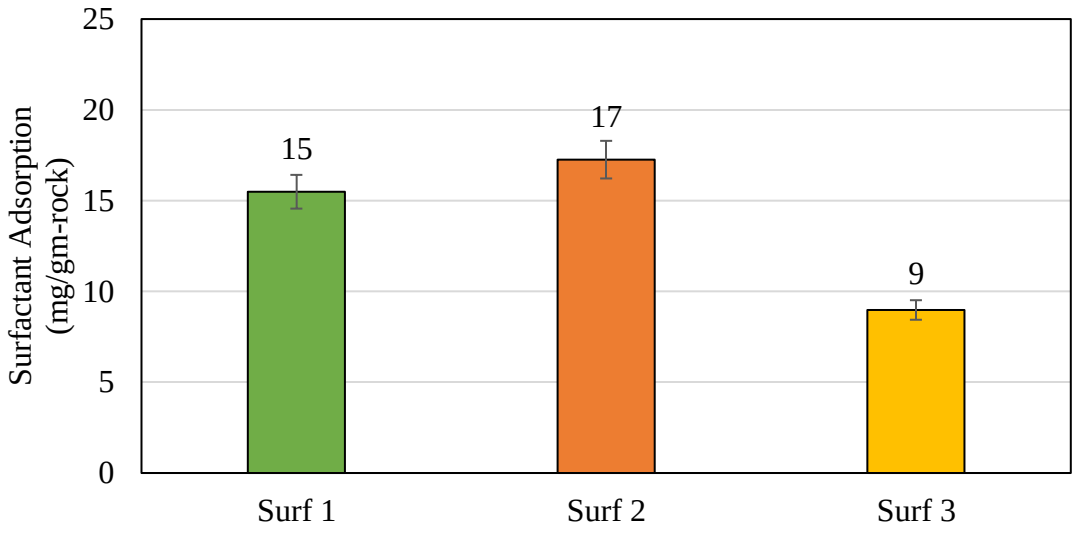



**Figure 23 - Surfactant adsorption results at 2 gpt concentration using UV-Vis spectrophotometer.**

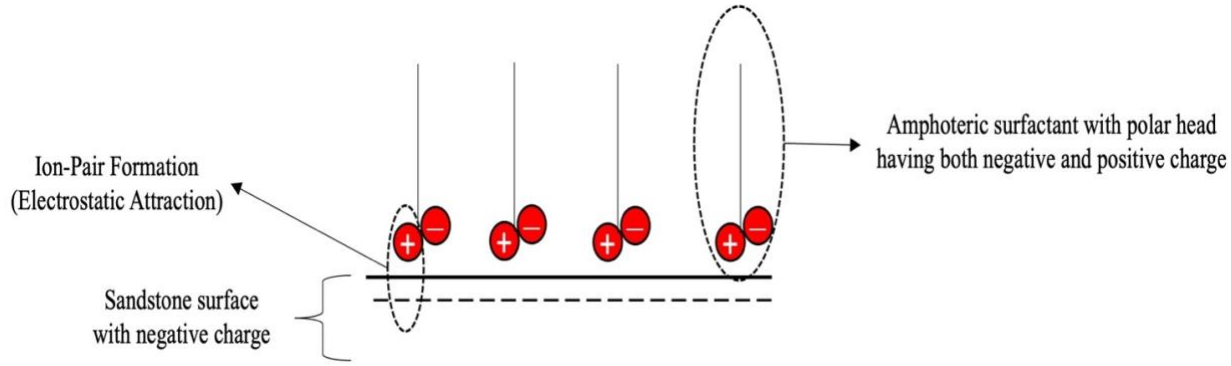



**Figure 24 - Model showing ion-pair formation between polar head of amphoteric surfactant and sandstone surface.**

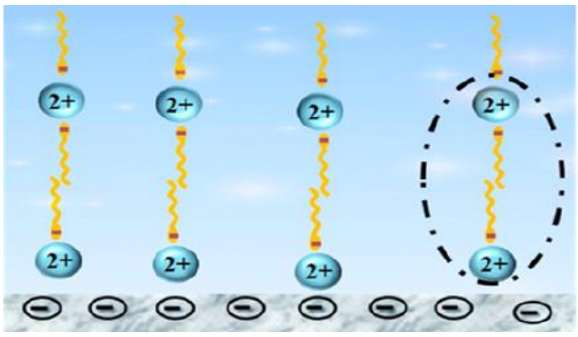



**Figure 25 - Adsorption of negative charged polar head of amphoteric surfactant to clay surface with $Ca^{2+}$ as a cationic bridge (Liu et al. 2021).**

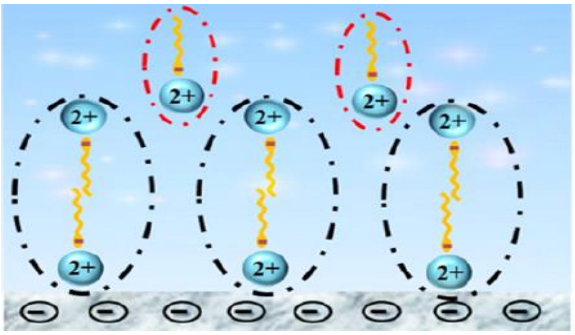



**Figure 26 - Excess $Ca^{2+}$ ions in surfactant solution creates multilayer of adsorped amphoteric surfactant (Liu et al. 2021).**

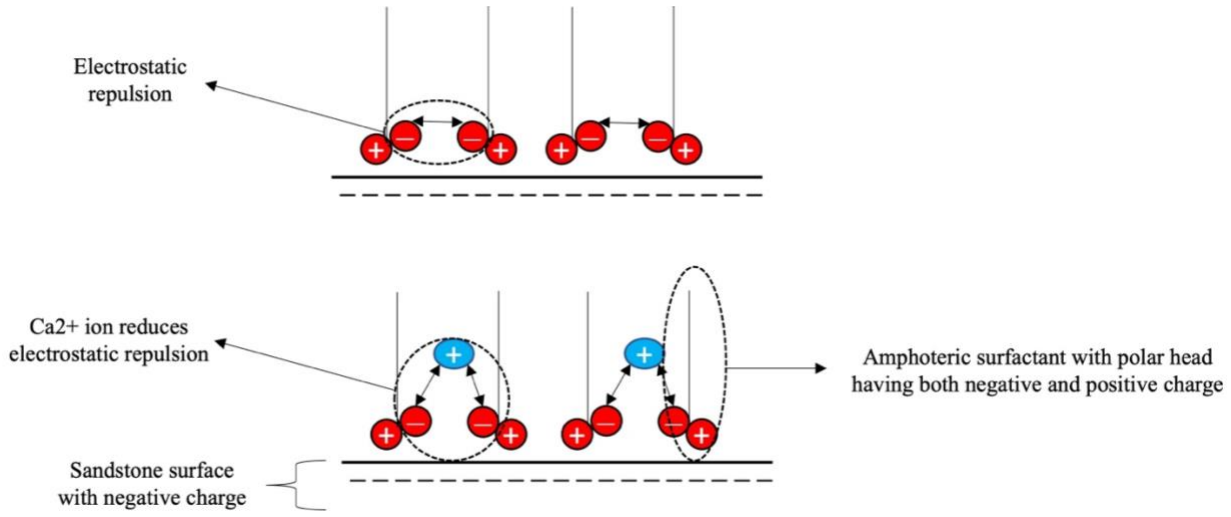



**Figure 27 - Model showing reduction in electrostatic repulsion between same charge on polar head of surfactants due to presence of divalent cations.**

### 4.5 Relationship between Surfactant Adsorption and Mineralogy

Results from surfactant adsorption measurements performed on five samples using surfactant at 2 gpt concentration are shown in Figure 28. Results here shows that surfactant 3 (biosurfactant) has much lower surfactant adsorption as compared to surfactant 1 and 2 (amphoteric). Also, results here show that divalent cations do not increase the reactivity of biosurfactant, and thus they are more stable at high TDS and temperature.

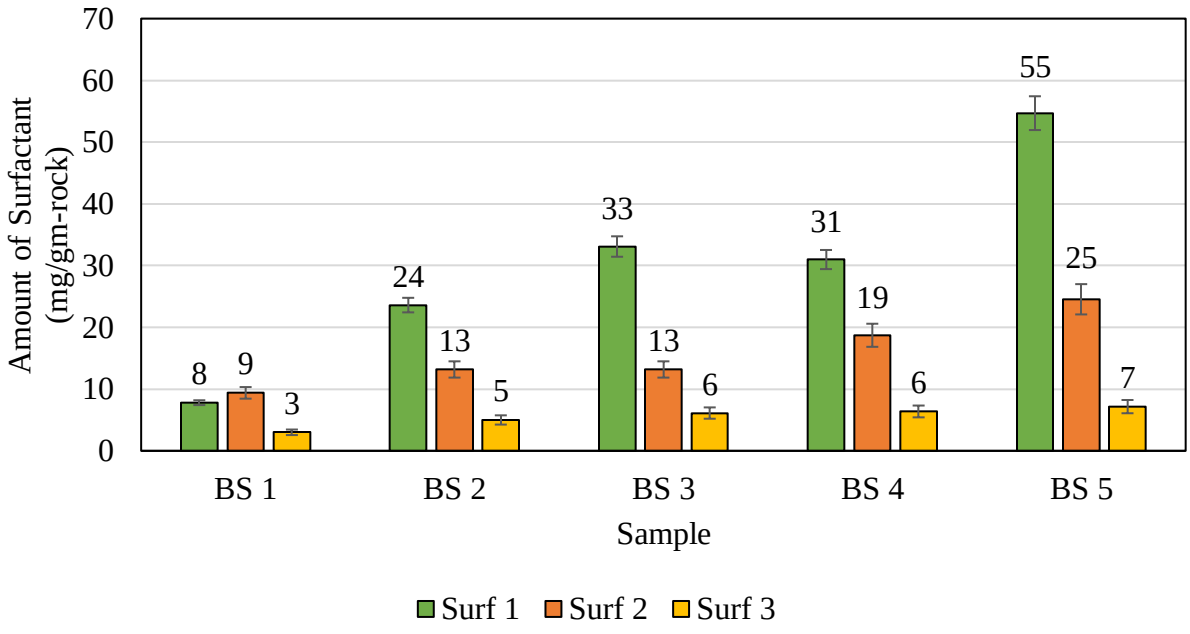



**Figure 28 - Surfactant adsorption results for five samples at 2 gpt concentration using UV-Vis spectrophotometer.**

#### 4.5.1 Surfactant Adsorption Relationship with Quartz plus Feldspars

Figure 29 presents the relationship between surfactant adsorption with quartz plus feldspars for the three surfactants. A negative linear trend was noticed with the surfactant adsorption and the minerals considered. This result shows that surfactant adsorption of amphoteric and biosurfactant depends on quartz plus feldspars concentration in sandstone reservoirs at high TDS and temperature.

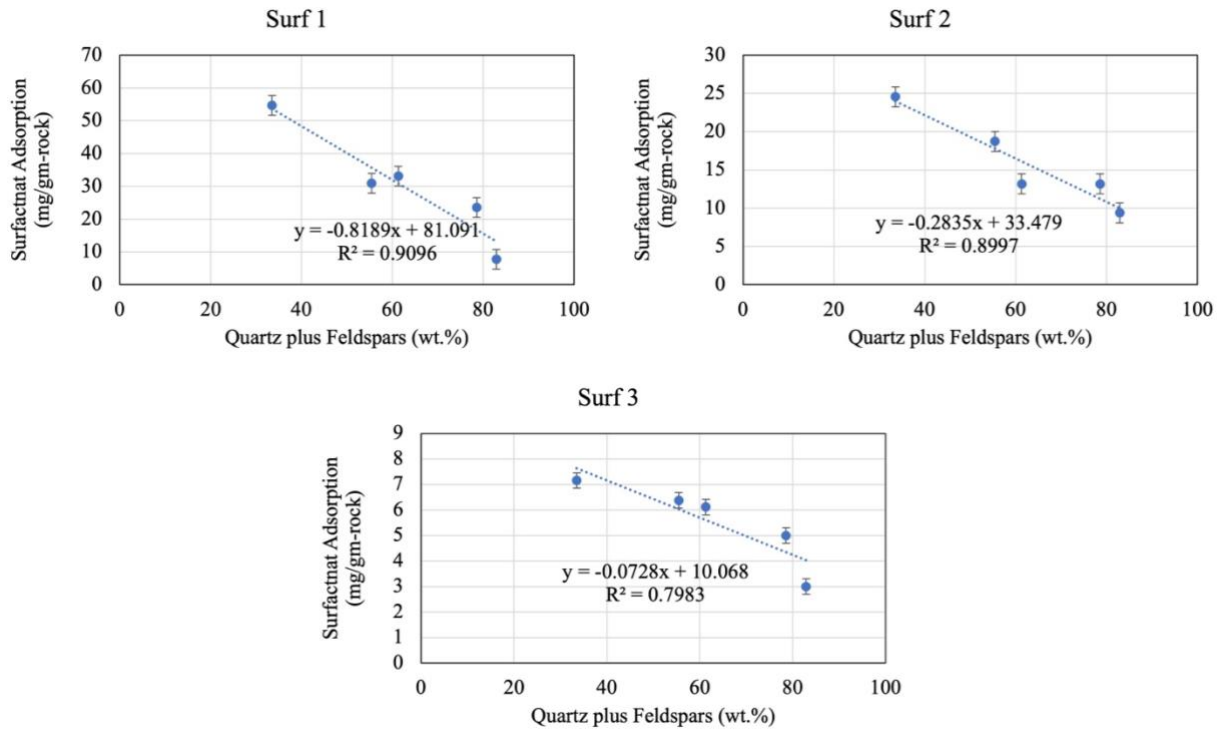



**Figure 29 - Relationship between amphoteric and biosurfactant adsorption with quartz plus feldspars in Bone Spring Sandstones.**

### 4.5.2 Surfactant Adsorption Relationship with Clays

Figure 30 presents the relationship between surfactant adsorption with total clays (illite plus mixed clays) for the three surfactants. A positive linear trend was observed with the surfactant adsorption and the mineral considered. This result shows that surfactant adsorption of amphoteric and biosurfactant depends on clay concentration in sandstone reservoirs at high TDS and temperature.

For amphoteric surfactant, this can be explained as with increase in clay percentage, negative charge on the rock surface increases. This validates our previous two hypotheses: adsorption of amphoteric surfactant and precipitation of divalent cations on negative charge clay surfaces. This leads to an increase in surfactant absorption.

For biosurfactants, increase in clays doesn't show increase in surfactant adsorption. It increases from 5 to 7 mg/gm-rock with increase in clays from 20 to 50 wt.%. This shows biosurfactant (glycolipids) can be used in reservoirs with higher TDS and temperature.

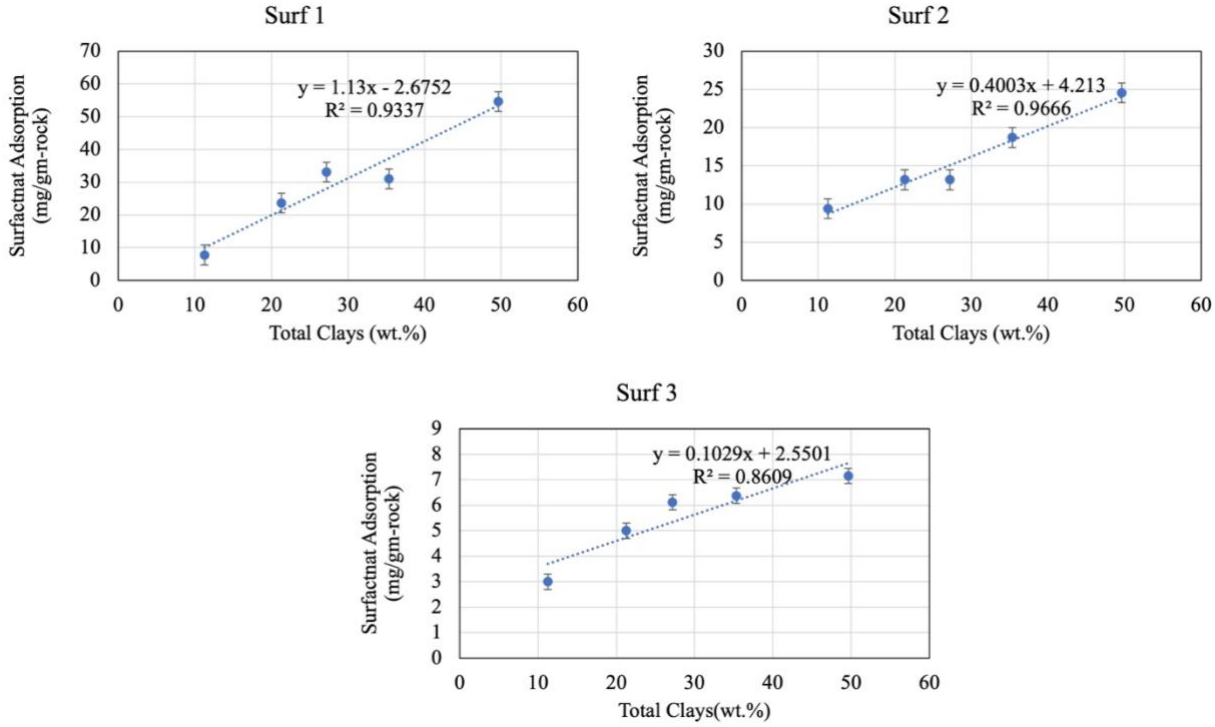



**Figure 30 - Relationship between amphoteric and biosurfactant adsorption with total clays (illite plus mixed clays) in Bone Spring sandstones.**

### 4.5.3 Surfactant Adsorption Relationship with Carbonates

Figure 31 presents the relationship between surfactant adsorption with total carbonates (dolomite and calcite) for the three surfactants. No observable trend was noticed with the surfactant adsorption and the minerals considered. This result shows that surfactant adsorption of amphoteric and biosurfactant does not depends on carbonate concentration in sandstone reservoirs at high TDS and temperature.

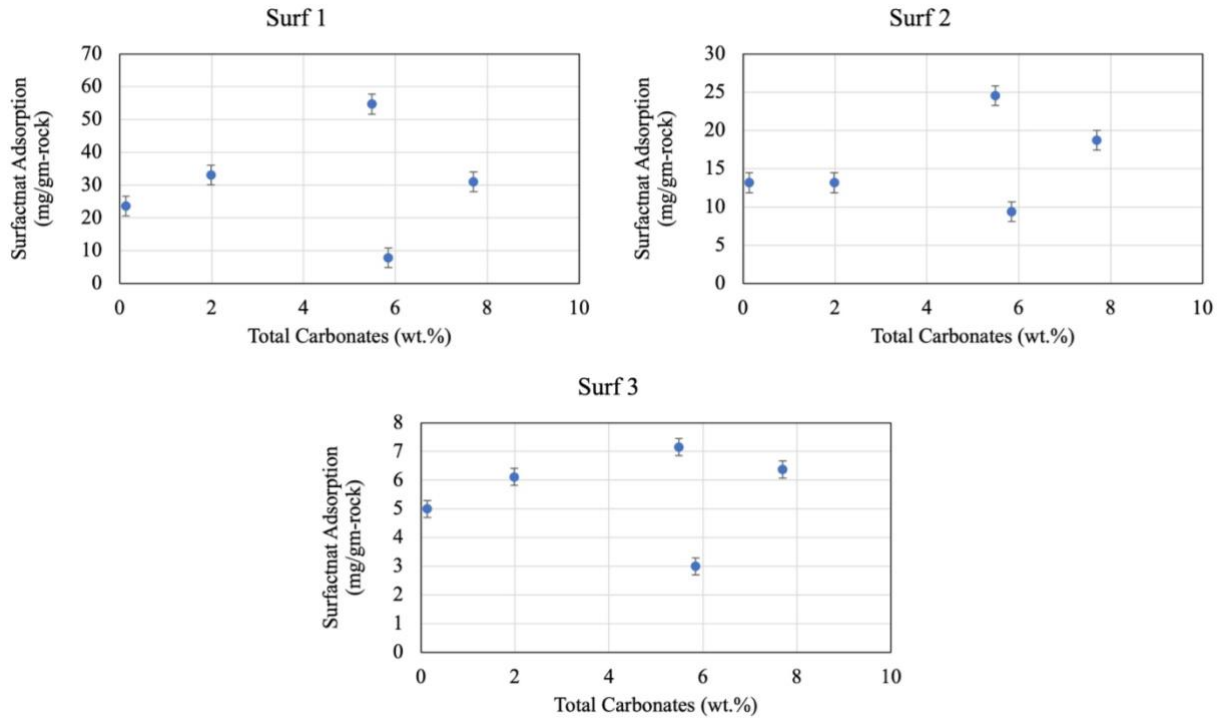



**Figure 31 - Relationship between amphoteric and biosurfactant adsorption with total carbonates (dolomite plus calcite) in Bone Spring sandstones.**

### 4.6 Imbibition Experiments using Produced Brine and Surfactants

As of now, we have seen that all three surfactant solutions reduce IFT and alter wettability. These changes modify the capillary pressure and generally increase the oil recovery. In this section, we quantity the oil recovery experimentally by repeatedly using same three sandstone samples with produced brine and three surfactants at 500 psi and 145 $^{o}$F. Initial baseline was established by calculating recovery using produced brine. After each surfactant imbibition, samples were cleaned, and recovery measurements were repeated using produced brine to ensure no alteration inside the plug from surfactant imbibition, as shown in Figure 7.

Figure 32 shows the oil recovery measured experimentally for three samples, while Figure 33 shows average of the oil recovery for produced brine and three surfactants. Results from imbibition of brine and surfactants showed that produced brine have 54% recovery of OOIP while

amphoteric surfactants have 45% and 41% recovery, which is lower than that of produced brine. Biosurfactant have the highest oil recovery with 60% of OOIP.

Here results indicate that rock/fluid interaction between sandstone surfaces and biosurfactant showed maximum alteration in wettability and made the rock surface most water wet compared to produced brine and amphoteric surfactants. Also, biosurfactant have the lowest IFT, with 96% reduction compared to produced brine. Wettability alteration and IFT reduction contributed to the highest oil recovery using biosurfactant at high TDS and temperature.

Lower oil recovery using amphoteric surfactants as compared to produced brine and biosurfactant again validates our previous two hypotheses: adsorption of amphoteric surfactant with positive charge polar head on negative charge clay surfaces and precipitation of divalent cations on negative charge clay surfaces. This precipitation further increases surfactant adsorption as divalent cations act as cationic bridge between amphoteric surfactants with negative charge polar heads and negative charge clay surfaces. Surfactant adsorption and precipitation of divalent cations together leads to a higher loss of surfactant from bulk solution to the rock surface, which blocks the movement of water into the rock sample giving oil recovery even lower than that of produced brine.

Results also indicate that divalent cations do not increase the reactivity between biosurfactant (glycolipids) and clay surface compared to amphoteric surfactants. Precipitation of divalent cations ions from the solution to rock surface is lower in biosurfactant than that of amphoteric surfactants, but there is some precipitation as oil recovery using biosurfactants is not much higher than produced brine. Table 8 summarizes the imbibition experiment results. Considering the economics, it might be more favorable to use only produced brine with no surfactant in a field-scale application.

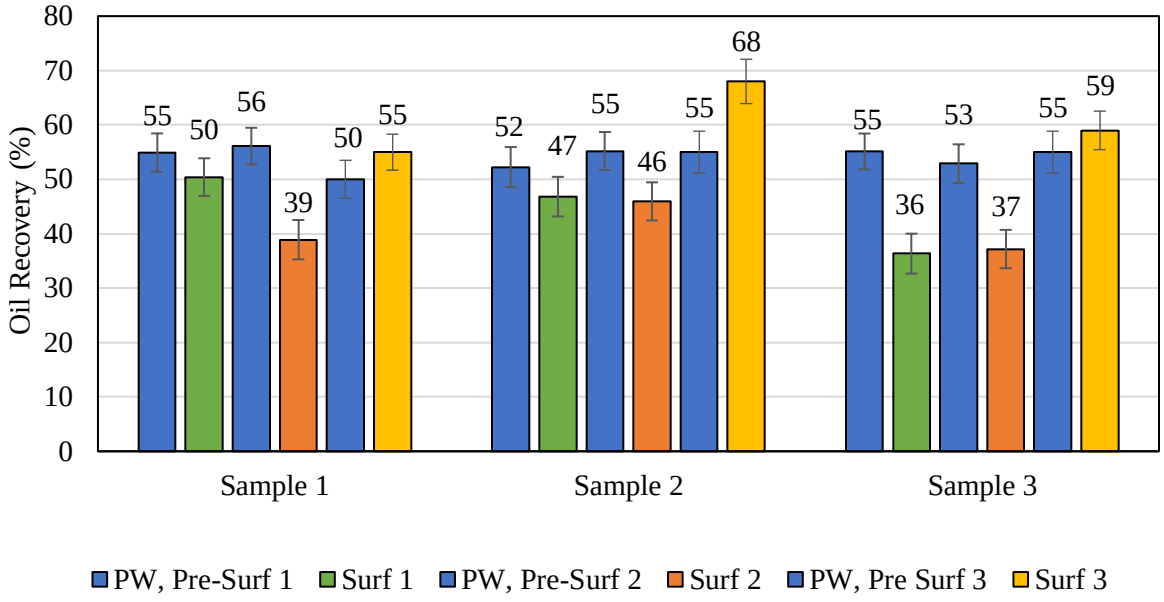



**Figure 32 - Oil recovery measured experimentally using imbibition of produced brine and surfactants at 2 gpt concentration in three Bone Spring sandstone samples at 500 psi and 145ºF. All three samples were exposed to brine and surfactants in a series of tests, as shown in Table 1. 12 MHz NMR was used to quantify the oil recovery by calculating the volume of oil inside the sample before and after imbibition.**

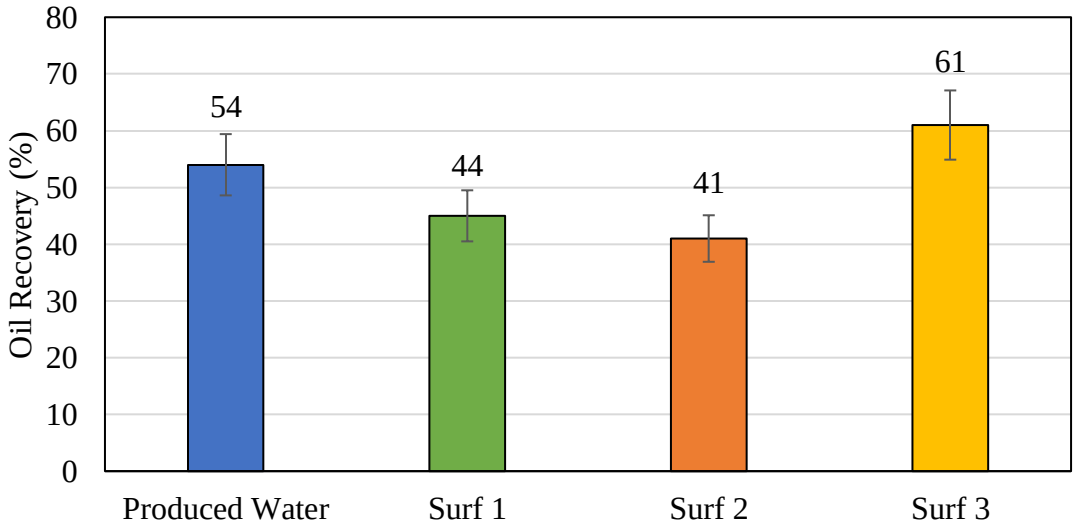



**Figure 33 - Average oil recovery measured experimentally using imbibition of produced brine and surfactants at 2 gpt concentration on three Bone Spring sandstone samples at 500 psi and 145ºF.**

| Fluid | Surfactant Type | IFT (mN/m) | Initial Contact Angle (degrees) | Final Contact Angle (degrees) | Surfactant Adsorption (mg/gm-rock) | Oil Recovery (%) |
|---|---|---|---|---|---|---|
| Produced Brine | – | 17.3 | 110 | 94 | – | 54 |
| Surfactant 1 | Amphoteric | 3.6 | 97 | 73 | 15 | 45 |
| Surfactant 2 | Amphoteric | 4.4 | 102 | 76 | 17 | 41 |
| Surfactant 3 | Biosurfactant | 0.7 | 92 | 55 | 9 | 61 |

**Table 8 - Summary of IFT, contact angle, surfactant adsorption, and oil recovery experiment results using produced brine and surfactants at 2 gpt concentration.**

# Chapter 5 : Conclusions, Surfactant Selection Strategy and Future Work Recommendations

## 5.1 Conclusions

Currently available literature lacks a study on the combined effect of IFT and wettability on oil recovery and surfactant adsorption on shaly sandstone. Literature is mainly focused on surfactant adsorption on pure minerals (clays and quartz), clean sandstones, and carbonates. Also, most surfactant testing using microbial surfactants have been done at low salinity and temperature. Though some studies claim that microbial surfactants work at high TDS and temperatures, no thorough experimental investigation have been done on plug samples. As well as there is a paucity of literature on sandstone with clays using amphoteric surfactants.

This study tried to close this gap by testing two amphoteric surfactants and one nonionic biosurfactant especially designed to be stable in reservoirs with high TDS and temperature on shaly sandstones. Following are the observations and conclusions which can be drawn from this study:

- Petrophysical analysis of plug samples used for imbibition experiments shows that the main constituents are quartz (41 to 54 wt.%) and clays (9 to 34 wt.%).
- Fluid/fluid interactions between crude oil and surfactants showed a reduction in IFT, with biosurfactant showing a maximum 95% reduction in IFT compared to produced brine.
- Rock/fluid interaction between rock samples and surfactants showed that the initial wettability of sandstone samples is oil-and-intermediate wet.
- All the surfactants alter wettability to water wet, but biosurfactant was the most effective.
- Surfactant adsorption measurements showed that amphoteric surfactants get strongly adsorbed, while biosurfactant showed the least adsorption on studied sandstone.

- For amphoteric surfactants, increase in clay concentration increased surfactant adsorption, which showed presence of clays is the main reason for higher surfactant adsorption. This was not observed for biosurfactant.
- With biosurfactant having low IFT, most reduction in wettability, and least surfactant adsorption, we see highest oil recovery, while amphoteric surfactants show approximately 16 to 24% lower oil recovery than produced brine due to loss of surfactants and precipitation of divalent cations from bulk volume to rock surface.
- This study shows that wettability and IFT alteration always do not favor higher oil recovery in shaly sandstone reservoirs with high TDS and temperature. Thoroughly performed lab experiments are required with plug samples, produced brine, and crude oil before using any type of surfactant for chemical EOR operation at well site.
- This study suggests that biosurfactant can be effectively used in Bone Spring sandstone with high TDS and temperature. Considering the economics, it might be more favorable to use only produced brine with no surfactant in a field-scale application.

### 5.2 Surfactant Selection Strategy for Sandstones

This study shows that a set of correlated laboratory experiments are required before using any surfactant for field trial. Below are the standardized experimental tests which we recommend on the basis of experimental observations and literature review on plug samples of 1 inch diameter and 1 to 2 inch thickness:

- Surfactant stability test at varying concentrations at reservoir and room temperature.
- CMC measurement of surfactant solution at reservoir temperature and salinity.
- IFT measurement of surfactant solution with crude oil and produced brine at reservoir and room temperature.

- Contact angle measurement of reservoir rock with surfactant solution and produced brine. First, after 100% oil saturation and second, after imbibition with surfactant solution and produced brine to measure wettability alteration.

IFT and contact angle measurements are the first order of tests that should be performed after surfactant stability and CMC measurement for every surfactant. These tests give us a first indication of which surfactant works the best.

- Zeta potential measurement to determine the affinity of produced brine and surfactant solution with rock surface
- Surfactant adsorption measurements to determine which surfactant shows the most surfactant adsorption on rock surface

Zeta Potential and surfactant adsorption measurements are the second order of tests that should be performed to study the interaction between the rock surface, produced brine, and surfactant solution. These tests give us a second indication of which surfactant works the best.

- At the end, imbibition experiments should be conducted using oil saturated plug samples at reservoir pressure and temperature to calculate the oil recovery.

Surfactant selection for field trial should be based on all the measurements from IFT, contact angle, zeta potential, surfactant adsorption, and imbibition experiment. Selection should never be skewed by seeing results from one experiment.

### 5.3 Future Work Recommendations

This section discusses recommendations for future work using surfactants to increase hydrocarbon recovery in shaly sandstones at high TDS and temperature:

- CMC measurements of surfactant solutions at reservoir temperature and salinity.

- Zeta potential measurements to determine the net charge on rock surface in presence of produced brine.
- TAN/TBN measurements to calculate the concentration of acidic/basic constituents of the crude oil.
- Cation Exchange Capacity (CEC) measurements along with UV Vis spectroscopy to understand surface chemistry and confirm cation precipitation, followed by excess surfactant adsorption is a function of mineralogy on the rock surface.
- Investigate the effect of cation precipitation on oil recovery in shaly sandstones by low salinity imbibition experiments.
- Develop a simulation model to understand ion pair formation and surfactant adsorption mechanisms between surfactant solution and oil wet sandstone surface with different types of clays, composite rock surfaces with different types of minerals along with presence of heavy hydrocarbon.

## References


1. Abdullah W., Buckley J., Carnegie A., Edwards J.J., Fordham E., Graue A., Habashy T., Hussain H., Mentaron B., and Ziauddin M., 2007. Fundamentals of Wettability. Oilfield Review, 19 (2): 44-61.
2. Ahmad M.T., 2020. Potential of Palm Kernel Alkanolamide Surfactant for Enhancing Oil Recovery from Sandstone Reservoir Rocks, Environment and Natural Resources Journal, Volume 18 (4). https://doi.org/10.5599/jese.2012.0026.
3. Ahmadi M.A., and Shadizadeh S.R., 2013. Experimental investigation of adsorption of a new nonionic surfactant on carbonate minerals, Fuel. 104, 462–467. https://doi.org/10.1016/j.fuel.2012.07.039.
4. Ahmadi M.A., Arabsahebi Y., Shadizadeh S.R., and Shokrollahzadeh S., 2014. Preliminary evaluation of mulberry leaf-derived surfactant on interfacial tension in an oil-aqueous system: EOR application, Fuel. 117, 749–755. https://doi.org/10.1016/j.fuel.2013.08.081.
5. Ali F.S.M., and Stahl C.D., 1970. *Increased oil recovery by improved waterflooding*. Earth Miner. Sci., United States. https://www.osti.gov/biblio/5001552
6. Alvarez J.O., Saputra I.W.R., and Schechter D.S., 2017. Potential of Improving Oil Recovery with Surfactant Additives to Completion Fluids for the Bakken, Energy & Fuels 31 (6): 5982–5994. https://doi.org/10.1021/acs.energyfuels.7b00573
7. Aminian A., and ZareNezhad B., 2019. Wettability alteration in carbonate and sandstone rocks due to low salinity Surfactant flooding, Journal of Molecular Liquids, Volume 275, Pages 265-280, ISSN 0167-7322. https://doi.org/10.1016/j.molliq.2018.11.080.

8. Anderson W.G., 1986. *Wettability Literature Survey—Part 2: Wettability Measurement*. J Pet Technol 38 (11):1246–1262. SPE-13933-PA
9. Atta D.Y., Negash B.M., and Yekeen N., 2021. A state-of-the art review on the application of natural Surfactants in enhanced oil recovery, Journal of Molecular Liquids, Volume 321, ISSN 0167-7322. https://doi.org/10.1016/j.molliq.2020.114888.
10. Atta D.Y., Negash B.M., Yekeen N., and Habte A.D., 2020. A state-of-the-art review on the application of natural Surfactants in enhanced oil recovery, Journal of Molecular Liquids, Volume 321, ISSN 0167-7322. https://doi.org/10.1016/j.molliq.2020.114888.
11. Ballard B.D., 2007. Quantitative Mineralogy of Reservoir Rocks Using Fourier Transform Infrared Spectroscopy. Paper presented at the SPE Annual Technical Conference and Exhibition, Anaheim, California, USA, 11–14 November. SPE-113023-STU. https://doi.org/10.2118/113023-STU.
12. Barati-Harooni A., Najafi-Marghmaleki S.M. and, Hosseini S, 2017. Experimental Investigation of Dynamic Adsorption–Desorption of New Nonionic Surfactant on Carbonate Rock: Application to Enhanced Oil Recovery, Journal of Energy Resources Technology139-42202. https://doi.org/10.1115/1.4036046.
13. Bashir A., Haddad A.S., and Rafati R., 2022. A review of fluid displacement mechanisms in surfactant-based chemical enhanced oil recovery processes: Analyses of key influencing factors, Petroleum Science, Volume 19, Issue 3, Pages 1211-1235, ISSN 1995-8226, https://doi.org/10.1016/j.petsci.2021.11.021.
14. Basu S., and Sharma M. M., 1997. *Characterization of Mixed-Wettability States in Oil Reservoirs by Atomic Force Microscopy*. SPE Journal 2 (04): 427-435.

15. Bataweel M.A., and Nasr-El-Din H.A., 2012. ASP vs. SP flooding in high salinity/hardness and temperature in sandstone cores, Paper presented at the SPE EOR Conference at Oil and Gas West Asia, Muscat, Oman, April 2012. https://doi.org/10.2118/155679-MS
16. Budhathoki M., Barnee S.H.R., Shiau B.J., and Harwell J.H., 2016. Improved oil recovery by reducing Surfactant adsorption with polyelectrolyte in high saline brine. Colloids and Surfaces A: Physicochemical and Engineering Aspects, Volume 498, Pages 66-73, ISSN 0927-7757. http://dx.doi.org/10.1016%2Fj.colsurfa.2016.03.012.
17. Camara J.M.D.A., Sousa M.A.S.B., Neto E.L.B., and Oilveira M.C.A., 2019. Application of rhamnolipid biosurfactant produced by Pseudomonas aeruginosa in microbial-enhanced oil recovery (MEOR). J Petrol Explor Prod Technol 9, 2333–2341. https://doi.org/10.1007/s13202-019-0633-x
18. Cheng Y., Yang Y., Niu C., Feng Z., Zhao W., and Lu S., 2019. Progress in synthesis and application of zwitterionic Gemini Surfactants. Frontiers of Material Science, 13, 242–257. https://doi.org/10.1007/s11706-019-0473-0
19. Dopfer O., 2006. Optical Spectroscopy in Chemistry and Life Sciences. An Introduction by Werner Schmidt Chem. Eur. J. of Chem. Phys., 7: 1598-1598. https://doi.org/10.1002/cphc.200600042.
20. Doust A.R., Puntervold T., and Austad T., 2011. Chemical verification of the EOR mechanism by using low saline/smart water in sandstone. Energy Fuels 25, 2151–2162. https://doi.org/10.1021/ef200215y.
21. Elraies K.A., Tan I.M., Awang M., and Saaid I., 2010. The synthesis and performance of sodium methyl ester sulfonate for enhanced oil recovery, Petroleum Science and Technology. 28, 1799–1806. https://doi.org/10.1080/10916460903226072.

22. Gannaway G., 2014. NMR Investigation of Pore Structure in Gas Shales. Paper presented at the SPE Annual Technical Conference and Exhibition. https://doi.org/10.2118/173474-STU.
23. Gomari S.R., Gomari, K.E., Islam M., and Hughes D., 2018. New Insight into the Influence of Rhamnolipid Bio-Surfactant on the Carbonate Rock/Water/Oil Interaction at Elevated Temperature. Resources 2018, 7, 75. https://doi.org/10.3390/resources7040075
24. Green D.W., and Willhite G.P., 1998. *Enhanced Oil Recovery*, SPE Textbook Series, Volume 6, Society of Petroleum Engineers, Richardson, Texas.
25. Gudina E.J., Rodrigues A.I., Alves E., Domingues M.R., Teixeira J.A, and Ligia R.R., 2015. Bioconversion of agro-industrial by-products in rhamnolipids toward applications in enhanced oil recovery and bioremediation, Bioresource Technology, Volume 177, Pages 87-93, ISSN 0960-8524. https://doi.org/10.1016/j.biortech.2014.11.069.
26. Gunther M., Zibek S., and Rupp S., 2017. Fungal Glycolipids as Biosurfactants, Current Biotechnology, Volume 6. http://dx.doi.org/10.2174/2211550105666160822170256.
27. Gupta R. and Mohanty K.K., 2008. Wettability alteration of fractured carbonate reservoirs. In: SPE Symposium on Improved Oil Recovery. Society of Petroleum Engineers, pp. 19–23. https://doi.org/10.2118/113407-MS.
28. Honciuc A., 2021. Chapter 4 - Surfactants and amphiphiles, Chemistry of Functional Materials Surfaces and Interfaces, Elsevier, Pages 43-77, ISBN 9780128210598. https://doi.org/10.1016/B978-0-12-821059-8.00011-9.
29. Ines M., and Dhouha G., 2015. Glycolipid Biosurfactants: Potential related biomedical and biotechnological applications, Carbohydrate Research, Volume 416, Pages 59-69, ISSN 0008-6215 https://doi.org/10.1016/j.carres.2015.07.016.

30. Ingrid H., 2014. Investigation of adsorption of surfactants onto illite and relations to enhanced oil recovery methods, MS Thesis, Norwegian University of Science and Technology (NTNU), Trondheim.
31. Jahan R., Bodratti A.M., Tsianou M., and Alexandridis P., 2020. Biosurfactants, natural alternatives to synthetic Surfactants: Physicochemical properties and applications. Adv. Colloid Interface Sci., 275, 102061. https://doi.org/10.1016/j.cis.2019.102061.
32. Kamal M.S., Hussain S.M.S., and Fogang L.T., 2019. Role of ionic headgroups on the thermal, rheological, and foaming properties of novel betaine-based polyoxyethylene zwitterionic Surfactants for enhanced oil recovery. Processes, 7(12), 908. https://doi.org/10.3390/pr7120908.
33. Kruss, 2022. Critical Micelle Concentration. (accessed November 20, 2022)
34. Kumar A., and Mandal A., 2019. Critical investigation of zwitterionic surfactant for enhanced oil recovery from both sandstone and carbonate reservoirs: Adsorption, wettability alteration and imbibition studies. Chemical Engineering Science, Volume 209, ISSN 0009-2509. https://doi.org/10.1016/j.ces.2019.115222.
35. Lake L.W., 1989. *Enhanced Oil Recovery, Chapter 9-Micellar-Polymer Flooding*, Upper Saddle River, NJ, 07458. Prentice-Hall Inc.
36. Law C., 1999. *Evaluating Source Rocks in Treatise of Petroleum Geology: Exploring for Oil and Gas Traps*, Chap. 6, 1–41. Special Publications, Tulsa, Oklahoma, USA: AAPG, ISBN 978-1-58861-493-3.
37. Lee K.S., and Lee J.J., 2019. *Chapter 2 - Mechanisms of Low-Salinity and Smart Waterflood, Hybrid Enhanced Oil Recovery using Smart Waterflooding*, Gulf Professional

Publishing, Pages 27-37, ISBN 9780128167762. https://doi.org/10.1016/B978-0-12-816776-2.00002-7

38. Liu Z., Ghatkesar M.K., Sudholter E.J., Singh B., and Kumar N., 2019. Understanding the cation dependent surfactant adsorption on clay minerals in oil recovery, Energy Fuel; 33(12):12319–29. https://doi.org/10.1021/acs.energyfuels.9b03109.
39. Liu Z., Ghatkesar M.K., Sudholter E.J.R., Binder Singh, and Kumar N., 2019. Understanding the Cation-Dependent Surfactant Adsorption on Clay Minerals in Oil Recovery, Energy & Fuels 2019 *33* (12), 12319-12329. 10.1021/acs.energyfuels.9b03109
40. Liu Z., Zhao G., Brewer M., Lv Q., and Sudholter E.J.R., 2021. Comprehensive review on surfactant adsorption on mineral surfaces in chemical enhanced oil recovery, Advances in Colloid and Interface Science, Volume 294, 102467, ISSN 0001-8686, https://doi.org/10.1016/j.cis.2021.102467.
41. Madani M., Zargar G., Takassi M.A., Daryasafar A., Wood D.A., and Zhang Z., 2019. Fundamental investigation of an environmentally-friendly surfactant agent for chemical enhanced oil recovery, Fuel. 238, 186–197. https://doi.org/10.1016/j.fuel.2018.10.105
42. Mannhardt K., Schramm L., and Novosad J., 1993. Effect of rock type and brine composition on adsorption of two foam-forming Surfactants. SPE Advanced Technical Series, Volume 1, p. 212-218. https://doi.org/10.2118/20463-PA.
43. Mantele W., and Deniz E., 2017. UV-VIS Absorption Spectroscopy: Lambert-Beer reloaded, Spectrochimica Acta Part A: Molecular and Biomolecular Spectroscopy, Volume 173, p. 965-968. https://doi.org/10.1016/j.saa.2016.09.037

44. Miller C., Bageri B.S., Zeng T., Patil S., and Mohanty K.K., 2020. Modified two-phase titration methods to quantify Surfactant concentrations in chemical-enhanced oil recovery applications. J. Surfactants Deterg. 23, 1159–1167. https://doi.org/10.1002/jsde.12442.
45. Mushtaq M., Tan I. M., Ismail L., Nadeem M., Sagir M., Azam R., and Hashmet R., 2014. Influence of PZC (Point of Zero Charge) on the Static Adsorption of Anionic Surfactants on a Malaysian Sandstone, Journal of Dispersion Science and Technology, 35:3, p. 343-349. https://doi.org/10.1080/01932691.2013.785362.
46. Saxena N., Pal N., Dey S., and Mandal A., 2017. Characterizations of surfactant synthesized from palm oil and its application in enhanced oil recovery, Journal of the Taiwan Institute of Chemical Engineers, 81, 343–355. https://doi.org/10.1016/j.jtice.2017.09.014.
47. Nowrouzi A.H., Mohammadi A.K., and Manshad, 2020. Characterization and evaluation of a natural surfactant extracted from Soapwort plant for alkali-surfactant-polymer (ASP) slug injection into sandstone oil reservoirs, Journal of Molecular Liquids. https://doi.org/10.1016/j.molliq.2020.114369.
48. Nowrouzi I., Mohammadi A.H., and Manshad A.K., 2021a. Chemical enhanced oil recovery by different scenarios of slug injection into carbonate/sandstone composite oil reservoirs using an anionic surfactant derived from rapeseed oil. Energy Fuels 35, 1248–1258. https://doi.org/10.1021/acs.energyfuels.0c03385.
49. Okoro E.E., Ewarezi E.A., Sanni S.E., Ojo T., Emertere M.E., and Omodara J.O., 2021. Microbial Enhanced Oil Recovery using Biosurfactant produced with Hyperthermophiles isolated from Subsurface Sandstone Reservoir, IOP Conf. Ser.: Earth Environ. Sci. 665 012062. 10.1088/1755-1315/665/1/012062

50. Paternina C.A., Londono A.K., Rondon M., Mercado R., and Botett J., 2020. Influence of salinity and hardness on the static adsorption of an extended surfactant for an oil recovery purpose. J. Pet. Sci. Eng. 195. https://doi.org/10.1016/j.petrol.2020.107592.
51. Paulino B.N., Pessoa M.G., Mano M.C., Molina G., and Neri-Numa I.A., Pastore G.M., 2016. Current status in biotechnological production and applications of glycolipid biosurfactants, Applied Microbiology and Biotechnology 100, 10265–93. https://doi.org/10.1007/s00253-016-7980-z.
52. Pillai P., and Mandal A., 2020. A comprehensive micro-scale study of poly-ionic liquid for application in enhanced oil recovery: Synthesis, characterization and evaluation of physicochemical properties, Journal of Molecular Liquids, 302, 112553. https://doi.org/10.1016/j.molliq.2020.112553.
53. Ravi S.G., Shadizadeh S.R., and Moghaddasi J., 2015. Core flooding tests to investigate the effects of IFT reduction and wettability alteration on oil recovery: Using mulberry leaf extract, Petroleum Science and Technology, 33, 257–264. https://doi.org/10.1080/10916466.2014.966916.
54. Saxena N., Kumar A., and Mandal, A., 2019. Adsorption analysis of natural anionic surfactant for enhanced oil recovery: The role of mineralogy, salinity, alkalinity, and nanoparticles. J. Petrol. Sci. Eng. 173, 1264–1283. http://dx.doi.org/10.1016/j.petrol.2018.11.002.
55. Schramm L.L., 2000. *Surfactants: Fundamentals and Applications in the Petroleum Industry*, Cambridge University Press, Cambridge, UK. http://dx.doi.org/10.2307/3515635

56. Shah D.O., and Schechter R.S., 1977. Improved oil recovery by surfactant and polymer flooding, AICHE Symposium on Improved Oil Recovery, Kansas City, Kansas. https://doi.org/10.1016/B978-0-126-41750-0.X5001-4

57. Sheng J.J., 2010. Optimum phase type and optimum salinity profile in surfactant flooding, Journal of Petroleum Science and Engineering, Volume 75, Issues 1–2, Pages 143-153, ISSN 0920-4105. https://doi.org/10.1016/j.petrol.2010.11.005.

58. Sondergeld C.H., and Rai C.S., 1993. A New Concept of Quantitative Core Characterization. Lead Edge 12 (7): 774–779. https://doi.org/10.1190/ 1.1436968.

59. Tiab D., and Donaldson E. C., 2012. Chapter 6 - Wettability, Petrophysics (Third Edition), Gulf Professional Publishing, Academic Pages 371-418, ISBN 9780123838483. https://doi.org/10.1016/B978-0-12-383848-3.00006-2.

60. Velioglu Z., and Urek R.O., 2015. Biosurfactant production by Pleurotus ostreatus in submerged and solid-state fermentation systems, Turkish Journal of Biology, Volume 39, Issue 1, Pages 160-166. https://doi.org/10.3906/biy-1406-44.

61. Walsh P., 2006. Geologic trends of oil and gas production in the Secretary of the Interior's Potash Area, Southeastern New Mexico, New Mexico Bureau of Geology and Mineral Resources.

62. Wang Y., Ge J., Zhang G., Jiang P., Zhang W., and Lin Y., 2015a. Adsorption behavior of dodecyl hydroxypropyl sulfobetaine on limestone in high salinity water. Rsc Adv. 5, 59738–59744. http://dx.doi.org/10.1039/c5ra10694j.

63. Wang Y., Xu H., and Yu W., 2011. Surfactant Induced Reservoir Wettability Alteration: Recent Theoretical and Experimental Advances in Enhanced Oil Recovery. Petroleum Science 8 (4): 463-476. https://doi.org/10.1007/s12182-011-0164-7.

64. Yekeen N., Malik A.A., Idris A.K., Reepei N.D., and Ganie K., 2020. Foaming properties, wettability alteration and interfacial tension reduction by saponin extracted from soapnut (Sapindus Mukorossi) at room and reservoir conditions, Journal of Petroleum Science and Engineering, Volume 195, ISSN 0920-4105 https://doi.org/10.1016/j.petrol.2020.107591.
65. Yekeen N., Malik A.A., Idris A.K., Reepei N.I., and Ganie K., 2020. Foaming properties, wettability alteration and interfacial tension reduction by saponin extracted from soapnut (Sapindus Mukorossi) at room and reservoir conditions, Journal of Petroleum Science and Engineering. 195. https://doi.org/10.1016/j.petrol.2020.107591.
66. Zeng T., Miller C. S., and Mohanty K., 2018. Applications of Surfactants in Shale Chemical EOR at High Temperatures. Paper presented at the SPE Improved Oil Recovery Conference, Tulsa, Oklahoma, USA, 14–18 April. SPE-190318-MS. https://doi.org/10.2118/190318-MS.
67. Zygler A., Słominska M., and Namiesnik J., 2012. Soxhlet Extraction and New Developments Such as Soxtec, Comprehensive Sampling and Sample Preparation, Academic Pages 65-82, ISBN 9780123813749. https://doi.org/10.1016/B978-0-12-381373-2.00037-5.